

Di-Higgs production as a probe of flavor changing neutral Yukawa couplings

Shi-Ping He(和世平)[†]

Center for Future High Energy Physics and Theoretical Physics Division, Institute of High Energy Physics,
Chinese Academy of Sciences, Beijing 100049, China

Abstract: Top partners are well motivated in many new physics models. Usually, vector like quarks, $T_{L,R}$, are introduced to circumvent the quantum anomaly. Therefore, it is crucial to probe their interactions with standard model particles. However, flavor changing neutral couplings are always difficult to detect directly in current and future experiments. In this paper, we demonstrate how to constrain the flavor changing neutral Yukawa coupling Tth indirectly, via the di-Higgs production. We consider the simplified model, including a pair of gauge singlet $T_{L,R}$. Under the perturbative unitarity and experimental constraints, we select $m_T = 400$ GeV, $s_L = 0.2$, and $m_T = 800$ GeV, $s_L = 0.1$ as benchmark points. After the analysis on the amplitude and evaluation of the numerical cross sections, we infer that the present constraints from di-Higgs production have already surpassed the unitarity bound because of the $(y_{L,R}^{tT})^4$ behavior. For the case of $m_T = 400$ GeV and $s_L = 0.2$, $\text{Re}y_{L,R}^{tT}$ and $\text{Im}y_{L,R}^{tT}$ can be bounded optimally in the range $(-0.4, 0.4)$ at the HL-LHC with 2σ CL. For the case of $m_T = 800$ GeV and $s_L = 0.1$, $\text{Re}y_{L,R}^{tT}$ and $\text{Im}y_{L,R}^{tT}$ can be bounded optimally in the range $(-0.5, 0.5)$ at the HL-LHC with 2σ CL. The anomalous triple Higgs coupling δ_{hhh} can also affect the constraints on $y_{L,R}^{tT}$. Finally, we determine that the top quark electric dipole moment can provide stronger $y_{L,R}^{tT}$ bounds in the off-axis regions for some scenarios.

Keywords: double Higgs, vector like quarks, flavour changing neutral Yukawa interactions

DOI: 10.1088/1674-1137/abfb50

I. INTRODUCTION

The standard model (SM) of elementary particle physics has been proposed for more than fifty years [1-3], and it is verified as a very effective description of this field [4]. The electro-weak symmetry breaking (EWSB) [5-8] mechanism predicts the existence of a physical Higgs boson, which is observed at the Large Hadron Collider (LHC) in 2012 [9, 10]. Although the SM is significantly strong, there are still a few unelucidated problems in particle physics. The typical problems are Higgs mass naturalness, gauge coupling unification, fermion mass hierarchy, electro-weak vacuum stability, dark matter, matter anti-matter asymmetry, etc. Many new physics beyond the SM (BSM) are aimed at solving or partially solving these problems. In some of these BSM models, vector-like quarks (VLQs) [11, 12] are introduced to circumvent the quantum anomaly.

For the up-type VLQ, the T quark can interact with the SM particles via the TbW , TtZ , and Tth interactions. Constraints on these couplings are crucial, because they can help us elucidate the nature of the EWSB. For the

strong interaction mediated pair production of VLQs, we can solely constrain the partial decay branching ratios of the T quark. To bound these couplings, the single production of VLQ needs to be considered. Unfortunately, it is difficult to directly detect the flavor changing neutral (FCN) interactions TtZ , Tth , owing to the suppression of the single T production from the tZ , th fusion. Here, we will focus on the FCN Yukawa (FCNY) interaction Tth . After the Higgs boson detection, we can obtain more information on new physics from the Higgs precision measurements [13-16]. The FCNY interaction can emerge in loop induced processes, for example, $h \rightarrow \gamma Z$ and $gg \rightarrow hh$. In our previous work [17], we demonstrated the possibility of constraining the FCNY coupling via the $h \rightarrow \gamma Z$ decay mode indirectly. The double Higgs production is also an appealing channel for elucidating the FCNY interaction, which is free of electro-weak gauge interactions. The constraints from $h \rightarrow \gamma Z$ and $gg \rightarrow hh$ are independent of exotic decay modes and total width of the T quark.

In this paper, we first discuss the framework of the developed FCN couplings in Sec. II. Sec. III is devoted to

Received 26 March 2021; Accepted 25 April 2021; Published online 10 June 2021

[†] E-mail: sphe@ihep.ac.cn

 Content from this work may be used under the terms of the Creative Commons Attribution 3.0 licence. Any further distribution of this work must maintain attribution to the author(s) and the title of the work, journal citation and DOI. Article funded by SCOAP³ and published under licence by Chinese Physical Society and the Institute of High Energy Physics of the Chinese Academy of Sciences and the Institute of Modern Physics of the Chinese Academy of Sciences and IOP Publishing Ltd

the theoretical and experimental constraints on the simplified model. In Sec. IV, we compute the new physics contributions to the parton level cross section of $gg \rightarrow hh$. Then we perform the numerical constraints on the FCNY interactions in Sec. V. Finally, we provide the summary and conclusions in Sec. VI.

II. FRAMEWORK OF FLAVOR CHANGING NEUTRAL COUPLINGS

A. Minimal singlet vector-like quark model

The SM gauge group is $SU_C(3) \otimes SU_L(2) \otimes U_Y(1)$, under which the singlet up-type VLQs have the representation $(3, 0, 2/3)$. Let us start with the minimal extension of SM by adding a pair of singlet T_L, T_R [11, 12], which is named as the VLQT model. Note that the mass mixing term $\bar{T}_L t_R$ can be discarded with field redefinition [18, 19]. Then, the Lagrangian can be written as [12]

$$\begin{aligned} \mathcal{L} &= \mathcal{L}_{\text{SM}} + \mathcal{L}_T^{\text{Yukawa}} + \mathcal{L}_T^{\text{gauge}}, \\ \mathcal{L}_T^{\text{Yukawa}} &= -\Gamma_T^i \bar{Q}_L^i \tilde{\Phi} T_R - M_T \bar{T}_L T_R + \text{h.c.}, \\ \mathcal{L}_T^{\text{gauge}} &= \bar{T}_L iD T_L + \bar{T}_R iD T_R, \end{aligned} \quad (1)$$

where $\tilde{\Phi} = i\sigma_2 \Phi^*$, and the covariant derivative is defined as $D_\mu = \partial_\mu - ig' Y_T B_\mu$. Y_T and Q_T are the $U_Y(1)$ and electric charge of the T quark, respectively. The Higgs

doublet is parametrized as $\Phi^T = \left[\phi^+, \frac{v+h+i\chi}{\sqrt{2}} \right]$. It is reasonable to ignore the mixings between heavy particles and the first two generations because of mass hierarchy and the bounds from flavor physics [20–22]. Here, for simplicity, we only consider the mixings between the third generation and heavy quarks.

To diagonalize the t and T quark mass terms, we can perform the transformations

$$\begin{aligned} \begin{bmatrix} t_L \\ T_L \end{bmatrix} &\rightarrow \begin{bmatrix} \cos\theta_L & \sin\theta_L \\ -\sin\theta_L & \cos\theta_L \end{bmatrix} \begin{bmatrix} t_L \\ T_L \end{bmatrix}, \\ \begin{bmatrix} t_R \\ T_R \end{bmatrix} &\rightarrow \begin{bmatrix} \cos\theta_R & \sin\theta_R \\ -\sin\theta_R & \cos\theta_R \end{bmatrix} \begin{bmatrix} t_R \\ T_R \end{bmatrix}. \end{aligned} \quad (2)$$

In fact, we obtain the relationship $m_T \tan\theta_R = m_t \tan\theta_L$. Subsequently, we will consider s_L, c_L, s_R, c_R as short forms for $\sin\theta_L, \cos\theta_L, \sin\theta_R, \cos\theta_R$, respectively. Then, we can obtain the mass eigenstate Yukawa interactions:

$$\begin{aligned} \mathcal{L}_{\text{Yukawa}} \supset &-m_t \bar{t}t - m_T \bar{T}T - \frac{m_t}{v} c_L^2 h \bar{t}t - \frac{m_T}{v} s_L^2 h \bar{T}T \\ &- \frac{m_T}{v} s_L c_L h (\bar{t}_L T_R + \bar{T}_R t_L) - \frac{m_t}{v} s_L c_L h (\bar{T}_L t_R + \bar{t}_R T_L), \end{aligned} \quad (3)$$

and gauge interactions

$$\begin{aligned} \mathcal{L}_{\text{gauge}} \supset &\frac{g}{c_W} Z_\mu \left[\left(\frac{1}{2} c_L^2 - \frac{2}{3} s_W^2 \right) \bar{t}_L \gamma^\mu t_L + \left(\frac{1}{2} s_L^2 - \frac{2}{3} s_W^2 \right) \bar{T}_L \gamma^\mu T_L + \frac{1}{2} s_L c_L (\bar{t}_L \gamma^\mu t_L + \bar{T}_L \gamma^\mu T_L) \right. \\ &\left. - \frac{2}{3} s_W^2 \bar{t}_R \gamma^\mu t_R - \frac{2}{3} s_W^2 \bar{T}_R \gamma^\mu T_R \right] + \frac{g c_L}{\sqrt{2}} (W_\mu^+ \bar{t}_L \gamma^\mu b_L + W_\mu^- \bar{b}_L \gamma^\mu t_L) + \frac{g s_L}{\sqrt{2}} (W_\mu^+ \bar{T}_L \gamma^\mu b_L + W_\mu^- \bar{b}_L \gamma^\mu T_L). \end{aligned} \quad (4)$$

Here, we have two independent extra parameters m_T and θ_L . For more details, please refer to our previous work [17].

B. Simplified model

In addition to the singlet VLQs, the scalar sector can be enlarged in the non-minimally extended models. For

example, we can also introduce a real gauge singlet scalar [23, 24], Higgs doublet [25], and even both the singlet-doublet scalars simultaneously [25, 26]. In these models, the T quark can possess other decay channels [27, 28]. Here, we will adopt a general framework [29]. Accordingly, the simplified related mass eigenstate interactions can be expressed as [17]

$$\begin{aligned} \mathcal{L} \supset &-m_t \bar{t}t - m_T \bar{T}T - e A_\mu \sum_{f=t,T} Q_f \bar{f} \gamma^\mu f + e Z_\mu \left[\bar{t} \gamma^\mu (g_L^t \omega_- + g_R^t \omega_+) t + \bar{T} \gamma^\mu (g_L^T \omega_- + g_R^T \omega_+) T \right. \\ &+ \bar{t} \gamma^\mu (g_L^{tT} \omega_- + g_R^{tT} \omega_+) T + \bar{T} \gamma^\mu (g_L^{tT} \omega_- + g_R^{tT} \omega_+) t \left. \right] - \frac{m_t}{v} h \bar{t} (\kappa_t + i \gamma^5 \tilde{\kappa}_t) t + h \bar{T} (y_T + i \gamma^5 \tilde{y}_T) T \\ &+ h \bar{t} (y_L^{tT} \omega_- + y_R^{tT} \omega_+) T + h \bar{T} (y_L^{tT})^* \omega_+ + (y_R^{tT})^* \omega_-) t + \frac{g c_L}{\sqrt{2}} (W_\mu^+ \bar{t}_L \gamma^\mu b_L + W_\mu^- \bar{b}_L \gamma^\mu t_L) \\ &+ \frac{g s_L}{\sqrt{2}} (W_\mu^+ \bar{T}_L \gamma^\mu b_L + W_\mu^- \bar{b}_L \gamma^\mu T_L) - \lambda_{hhh} h^3, \end{aligned} \quad (5)$$

where ω_{\pm} are the chirality projection operators $(1 \pm \gamma^5)/2$ and the gauge couplings are presented as

$$\begin{aligned} g_L^t &= \frac{1}{s_W c_W} \left(\frac{1}{2} c_L^2 - \frac{2}{3} s_L^2 \right), \quad g_L^T = \frac{1}{s_W c_W} \left(\frac{1}{2} s_L^2 - \frac{2}{3} c_L^2 \right), \\ g_L^{tT} &= \frac{s_L c_L}{2 s_W c_W}, \quad g_R^t = -\frac{2 s_W}{3 c_W}, \quad g_R^T = -\frac{2 s_W}{3 c_W}, \quad g_R^{tT} = 0. \end{aligned} \quad (6)$$

The triple Higgs coupling λ_{hhh} can deviate from the SM value $\lambda_{hhh}^{\text{SM}} = \frac{m_h^2}{2\nu}$ in many new physics models [30-39]. Here, m_T , θ_L , κ_t , $\tilde{\kappa}_t$, y_T , \tilde{y}_T are all real parameters, while y_L^{tT} , y_R^{tT} can be complex. Henceforth, we will turn off the parameters $\tilde{\kappa}_t$ and \tilde{y}_T for simplicity.

Next, we will demonstrate how to constrain the FCNY couplings via the $gg \rightarrow hh$ channel. Although the FCNY couplings $y_{L,R}^{tT}$ are not free parameters in the above VLQT model, they can be free in more complex models. If we can extend the SM by the singlet T_L , T_R and many new scalars, there can be enough degrees of freedom. Therefore, we can consider them as free parameters in realizing a general analysis.

III. CONSTRAINTS ON THE SIMPLIFIED MODEL

In this section, we will review the theoretical and experimental constraints on the simplified model. Specific details can be obtained from our previous study [17]. The S-wave unitarity will lead to the bound [17]

$$\sqrt{(|y_L^{tT}|^2 + |y_R^{tT}|^2)^2 + 12|y_L^{tT}|^2|y_R^{tT}|^2} + |y_L^{tT}|^2 + |y_R^{tT}|^2 \leq 16\pi. \quad (7)$$

In Fig. 1, we present the unitarity allowed region in the plane of $|y_L^{tT}| - |y_R^{tT}|$. Higgs signal strength and top quark physics provide relatively loose constraints. Direct search can bound the VLQ mass as light as 400 GeV without specific assumptions [28]. The strongest constraints on m_T and s_L originate from the electro-weak precision measurements. Here, we consider the S and T parameters [22, 40-43]. In Fig. 2, we present the allowed parameter space regions from the global fits at 1σ and 2σ confidence levels (CLs). In this study, the input parameters are selected as $m_Z = 91.1876$ GeV, $m_W = 80.387$ GeV, $m_h = 125.09$ GeV, $m_t = 172.74$ GeV, $G_F = 1.1664 \times 10^{-5}$ GeV $^{-2}$, and $c_W = m_W/m_Z$ [4].

Next, we consider the constraints from the top quark electric dipole moment (EDM). If CP violation exists in the FCNY interactions, it will contribute to the EDM type interaction $-\frac{i}{2} d_t^{\text{EDM}} \bar{t} \sigma^{\mu\nu} \gamma^5 t F_{\mu\nu}$. The d_t^{EDM} is calculated as

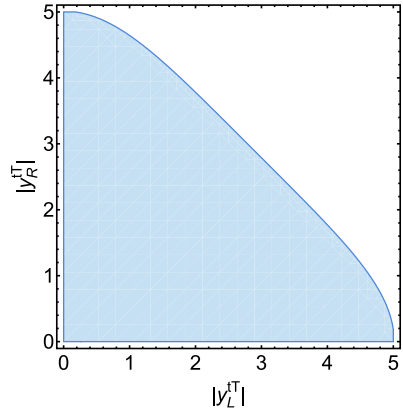


Fig. 1. (color online) Parameter region allowed by the perturbative unitarity. Figure from Ref. [17].

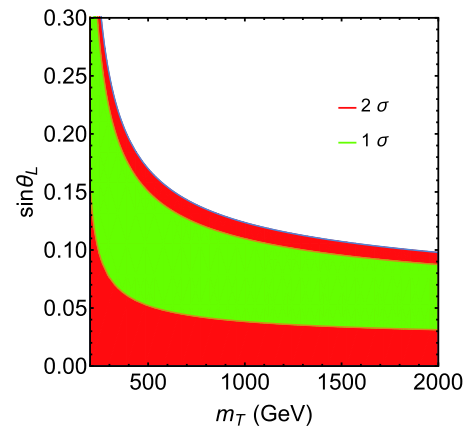


Fig. 2. (color online) Constraints on m_T , s_L from the S and T parameters. Here, the green and red colors depict the allowed regions at 1σ and 2σ CLs, respectively. Figure from Ref. [17].

$$d_t^{\text{EDM}} = \frac{e Q_T m_T [y_R^{tT} (y_L^{tT})^* - y_L^{tT} (y_R^{tT})^*]}{16\pi^2 i} C_1, \quad (8)$$

with C_1 defined as

$$\begin{aligned} C_1 = & \frac{1}{4m_t^2} [B_0(m_t^2, m_T^2, m_h^2) - B_0(0, m_T^2, m_T^2) \\ & + (m_T^2 - m_t^2 - m_h^2) C_0(m_t^2, 0, m_t^2, m_h^2, m_T^2, m_T^2)]. \end{aligned}$$

As can be observed from the identity $[y_R^{tT} (y_L^{tT})^* - y_L^{tT} (y_R^{tT})^*] = 2i(\text{Re} y_L^{tT} \text{Im} y_R^{tT} - \text{Re} y_R^{tT} \text{Im} y_L^{tT})$, d_t^{EDM} will vanish if we turn off both the imaginary parts of $y_{L,R}^{tT}$. The top quark EDM can be bounded as $|d_t^{\text{EDM}}| < 5 \times 10^{-20} e \cdot \text{cm}$ at 90% CL [44-46] with the ACME results [47]. In fact, we can rescale the limit to be $|d_t^{\text{EDM}}| < 6.3 \times 10^{-21} e \cdot \text{cm}$ or $|m_t d_t^{\text{EDM}}/e| < 5.5 \times 10^{-5}$ with the improved data [17, 48]. If we consider $m_T = 400$ GeV, the top EDM sets the upper limit of $|y_R^{tT} (y_L^{tT})^* - y_L^{tT} (y_R^{tT})^*|$ to be 0.12 at 90% CL. If we take $m_T = 800$ GeV, the corresponding upper limit of $|y_R^{tT} (y_L^{tT})^* - y_L^{tT} (y_R^{tT})^*|$ is 0.24 at 90% CL. The looseness of

the constraints increases with m_T .

IV. ANALYSIS OF DOUBLE HIGGS PRODUCTION

A. New physics results on amplitude

The double Higgs production is a trending topic in the field of Higgs physics. The di-Higgs production cross section has been calculated in SM for several years [49, 50]. The new physics effects have also garnered considerable attention in this community [51-55]. A few studies on di-Higgs production are based on the SM effective field theory (EFT) [56-61] and non-linearly realized EFT [62-65]. There are also several studies considered in specific models, such as the Higgs singlet model [66-68], two Higgs doublet model [69-72], VLQ models [73-75], composite Higgs models [76, 77], minimal supersymmetric standard model (MSSM) [78-80], next-to-MSSM [81, 82], and many other new physics models.

For VLQ models, there are additional fermion contributions: the pure new quark loops and loops with both SM and new quarks. In Figs. 3 and 4, we present the Feynman diagrams from the pure quark loops and mixed quark loops, respectively¹⁾. The latter will be induced by FCNY interactions. The FCNY contributions are less considered in most studies, as they are smaller than the same flavor terms. However, this channel can be sensitive to large FCNY couplings.

Starting from the Lagrangian in Eq. (5), the amplitude of $gg \rightarrow hh$ can be parametrized as

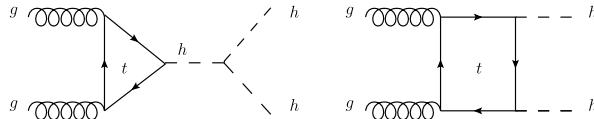


Fig. 3. Typical Feynman diagrams contributing to the $g(k_1, \mu)g(k_2, \nu) \rightarrow h(p_1)h(p_2)$ production with pure top (and T) quarks running in the loops, where the counter-clockwise diagrams should be included.

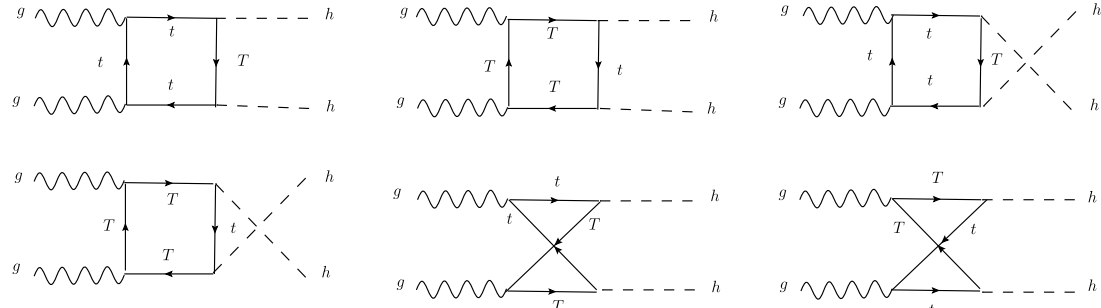


Fig. 4. Typical Feynman diagrams contributing to the $g(k_1, \mu)g(k_2, \nu) \rightarrow h(p_1)h(p_2)$ production with both top and T quarks running in the loops, where the counter-clockwise diagrams should be included.

1) The diagrams are drawn by JaxoDraw [83].

2) During the calculations, we have used the FeynCalc to simplify the results [84, 85].

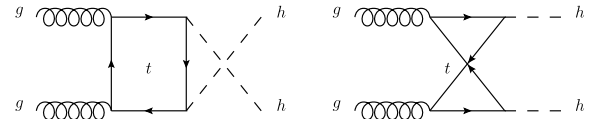
$$i\mathcal{M}(\hat{s}) = -i \frac{g_s^2 \hat{s}}{16\pi^2 v^2} \epsilon_{\mu}^{a,r_1}(k_1) \epsilon_{\nu}^{a,r_2}(k_2) (A^{\mu\nu} f_A + B^{\mu\nu} f_B + C^{\mu\nu} f_C), \quad (9)$$

where a and $r_{1,2}$ represent the color and spin indices, respectively, and the tensor structures $A^{\mu\nu}$, $B^{\mu\nu}$, $C^{\mu\nu}$ are given by

$$\begin{aligned} A^{\mu\nu} &\equiv g^{\mu\nu} - \frac{k_2^\mu k_1^\nu}{k_1 \cdot k_2}, & C^{\mu\nu} &\equiv \frac{k_{1\rho} k_{2\sigma} \epsilon^{\mu\nu\rho\sigma}}{k_1 \cdot k_2}, \\ B^{\mu\nu} &\equiv g^{\mu\nu} + \frac{m_h^2 k_2^\mu k_1^\nu}{p_T^2 (k_1 \cdot k_2)} - \frac{2(k_1 \cdot p_1) k_2^\mu p_1^\nu}{p_T^2 (k_1 \cdot k_2)} - \frac{2(k_2 \cdot p_1) p_1^\mu k_1^\nu}{p_T^2 (k_1 \cdot k_2)} \\ &\quad + \frac{2p_1^\mu p_1^\nu}{p_T^2} \quad (p_T^2 \equiv \frac{\hat{m}_h^2 - m_h^4}{\hat{s}}). \end{aligned} \quad (10)$$

These structures possess the orthonormal relationships $A^{\mu\nu} A_{\mu\nu} = B^{\mu\nu} B_{\mu\nu} = C^{\mu\nu} C_{\mu\nu} = 2$ and $A^{\mu\nu} B_{\mu\nu} = A^{\mu\nu} C_{\mu\nu} = B^{\mu\nu} C_{\mu\nu} = 0$. The coefficients $f_{A,B,C}$ receive contributions from the t and T quark loops and can be written as $f_{A,B,C} \equiv f_{A,B,C}^t + f_{A,B,C}^T + f_{A,B,C}^{tT}$. Here, $f_{A,B,C}^{t(T)}$ represents the contributions from pure t (T) quark loops, while $f_{A,B,C}^{tT}$ indicate the contributions from mixed t and T quark loops. When we set $\kappa_t^2 = 1$ and turn off the couplings $y_{L,R}^T$, they move straight to the SM result. After a few lengthy calculations, we can obtain their explicit expressions.

The pure top quark contribution to f_A is given by²⁾ $f_A^t = \kappa_t f_A^{t,\Delta} + \kappa_t^2 f_A^{t,\square 1}$. Here, $f_A^{t,\Delta}$ and $f_A^{t,\square 1}$ are defined as



$$\begin{aligned} f_A^{t,\Delta} &= \frac{6m_h^2 m_t^2}{\hat{s}(\hat{s}-m_h^2)} \left[2 + (4m_t^2 - \hat{s})C_0^t(\hat{s}) \right], \\ f_A^{t,\square 1} &= \frac{2m_t^2}{\hat{s}} \left\{ 4m_t^2 C_0^t(\hat{s}) + \frac{2(m_h^2 - 4m_t^2)}{\hat{s}} \left[(\hat{t} - m_h^2)C_0^t(\hat{t}) \right. \right. \\ &\quad \left. \left. + (\hat{u} - m_h^2)C_0^t(\hat{u}) \right] + m_t^2(8m_t^2 - \hat{s} - 2m_h^2) \right. \\ &\quad \times \left[D_0^t(\hat{t}, \hat{s}) + D_0^t(\hat{u}, \hat{s}) + D_0^t(\hat{t}, \hat{u}) \right] \\ &\quad \left. + 2 + \frac{\hat{t}\hat{u} - m_h^4}{\hat{s}}(4m_t^2 - m_h^2)D_0^t(\hat{t}, \hat{u}) \right\}. \end{aligned} \quad (11)$$

The pure T quark contribution to f_A is given by $f_A^T = \left(-\frac{vy_T}{m_T}\right)f_A^{T,\Delta} + \left(\frac{vy_T}{m_T}\right)^2 f_A^{T,\square 1}$. Here, $f_A^{T,\Delta}$ and $f_A^{T,\square 1}$ are defined as

$$\begin{aligned} f_A^{T,\Delta} &= \frac{6m_h^2 m_T^2}{\hat{s}(\hat{s}-m_h^2)} \left[2 + (4m_T^2 - \hat{s})C_0^T(\hat{s}) \right], \\ f_A^{T,\square 1} &= \frac{2m_T^2}{\hat{s}} \left\{ 4m_T^2 C_0^T(\hat{s}) + \frac{2(m_h^2 - 4m_T^2)}{\hat{s}} \left[(\hat{t} - m_h^2)C_0^T(\hat{t}) \right. \right. \\ &\quad \left. \left. + (\hat{u} - m_h^2)C_0^T(\hat{u}) \right] + m_T^2(8m_T^2 - \hat{s} - 2m_h^2) \right. \\ &\quad \times \left[D_0^T(\hat{t}, \hat{s}) + D_0^T(\hat{u}, \hat{s}) + D_0^T(\hat{t}, \hat{u}) \right] \\ &\quad \left. + 2 + \frac{\hat{t}\hat{u} - m_h^4}{\hat{s}}(4m_T^2 - m_h^2)D_0^T(\hat{t}, \hat{u}) \right\}. \end{aligned} \quad (12)$$

The top and T quark mixed contributions to f_A is given by $f_A^{tT} = (|y_L^{tT}|^2 + |y_R^{tT}|^2)f_A^{tT,\square 1} + [y_L^{tT}(y_R^{tT})^* + y_R^{tT}(y_L^{tT})^*]f_A^{tT,\square 2}$. Here, $f_A^{tT,\square 1}$ and $f_A^{tT,\square 2}$ are defined as:

$$\begin{aligned} f_A^{tT,\square 1} &= \frac{2v^2}{\hat{s}} \left\{ 2m_t^2 C_0^t(\hat{s}) + 2m_T^2 C_0^T(\hat{s}) + \frac{m_h^2 - m_t^2 - m_T^2}{\hat{s}} \left[(\hat{t} - m_h^2)(C_0^{tT}(\hat{t}) + C_0^{Tt}(\hat{t})) + (\hat{u} - m_h^2)(C_0^{tT}(\hat{u}) + C_0^{Tt}(\hat{u})) \right] \right. \\ &\quad \left. + (m_t^2 + m_T^2 - m_h^2) \left[m_t^2(D_0^{tT}(\hat{t}, \hat{s}) + D_0^{tT}(\hat{u}, \hat{s}) + D_0^{tT}(\hat{t}, \hat{u})) + m_T^2(D_0^{Tt}(\hat{t}, \hat{s}) + D_0^{Tt}(\hat{u}, \hat{s}) + D_0^{Tt}(\hat{t}, \hat{u})) \right] \right. \\ &\quad \left. + 2 + \frac{\hat{t}\hat{u} - m_h^4}{\hat{s}}(m_t^2 + m_T^2 - m_h^2)D_0^{tT}(\hat{t}, \hat{u}) \right\}, \\ f_A^{tT,\square 2} &= \frac{m_t m_T v^2}{\hat{s}^2} \left\{ 4(m_h^2 - \hat{t}) \left[C_0^{tT}(\hat{t}) + C_0^{Tt}(\hat{t}) \right] + 4(m_h^2 - \hat{u}) \left[C_0^{tT}(\hat{u}) + C_0^{Tt}(\hat{u}) \right] \right. \\ &\quad \left. + \hat{s}(4m_t^2 - \hat{s}) \left[D_0^{tT}(\hat{t}, \hat{s}) + D_0^{tT}(\hat{u}, \hat{s}) + D_0^{tT}(\hat{t}, \hat{u}) \right] + \hat{s}(4m_T^2 - \hat{s}) \left[D_0^{Tt}(\hat{t}, \hat{s}) + D_0^{Tt}(\hat{u}, \hat{s}) + D_0^{Tt}(\hat{t}, \hat{u}) \right] \right. \\ &\quad \left. + 4(\hat{t}\hat{u} - m_h^4)D_0^{tT}(\hat{t}, \hat{u}) \right\}. \end{aligned} \quad (13)$$

The pure top quark contribution to f_B is given by $f_B^t = \kappa_t^2 f_B^{t,\square 1}$. Here, $f_B^{t,\square 1}$ is defined as

$$\begin{aligned} f_B^{t,\square 1} &= \frac{m_t^2}{\hat{s}} \left\{ -2\hat{s}C_0^t(\hat{s}) + 2(m_h^2 - \hat{t})C_0^t(\hat{t}) + 2(m_h^2 - \hat{u})C_0^t(\hat{u}) - 2(8m_t^2 + \hat{s} - 2m_h^2)C_0^t(m_h^2) \right. \\ &\quad + 2m_t^2(8m_t^2 + \hat{s} - 2m_h^2) \left[D_0^t(\hat{t}, \hat{s}) + D_0^t(\hat{u}, \hat{s}) + D_0^t(\hat{t}, \hat{u}) \right] \\ &\quad + \frac{1}{\hat{t}\hat{u} - m_h^4} \left[\hat{s}\hat{t}(8m_t^2\hat{t} - \hat{t}^2 - m_h^4)D_0^t(\hat{t}, \hat{s}) + \hat{s}\hat{u}(8m_t^2\hat{u} - \hat{u}^2 - m_h^4)D_0^t(\hat{u}, \hat{s}) \right. \\ &\quad \left. + (8m_t^2 + \hat{s} - 2m_h^2) \left(\hat{s}(\hat{s} - 2m_h^2)C_0^t(\hat{s}) + \hat{s}(\hat{s} - 4m_h^2)C_0^t(m_h^2) + 2\hat{t}(m_h^2 - \hat{t})C_0^t(\hat{t}) + 2\hat{u}(m_h^2 - \hat{u})C_0^t(\hat{u}) \right) \right\}. \end{aligned} \quad (14)$$

The pure T quark contribution to f_B is given by $f_B^T = \left(\frac{vy_T}{m_T}\right)^2 f_B^{T,\square 1}$. Here, $f_B^{T,\square 1}$ is defined as

$$\begin{aligned} f_B^{T,\square 1} &= \frac{m_T^2}{\hat{s}} \left\{ -2\hat{s}C_0^T(\hat{s}) + 2(m_h^2 - \hat{t})C_0^T(\hat{t}) + 2(m_h^2 - \hat{u})C_0^T(\hat{u}) - 2(8m_T^2 + \hat{s} - 2m_h^2)C_0^T(m_h^2) \right. \\ &\quad + 2m_T^2(8m_T^2 + \hat{s} - 2m_h^2) \left[D_0^T(\hat{t}, \hat{s}) + D_0^T(\hat{u}, \hat{s}) + D_0^T(\hat{t}, \hat{u}) \right] \\ &\quad + \frac{1}{\hat{t}\hat{u} - m_h^4} \left[\hat{s}\hat{t}(8m_T^2\hat{t} - \hat{t}^2 - m_h^4)D_0^T(\hat{t}, \hat{s}) + \hat{s}\hat{u}(8m_T^2\hat{u} - \hat{u}^2 - m_h^4)D_0^T(\hat{u}, \hat{s}) \right. \\ &\quad \left. + (8m_T^2 + \hat{s} - 2m_h^2) \left(\hat{s}(\hat{s} - 2m_h^2)C_0^T(\hat{s}) + \hat{s}(\hat{s} - 4m_h^2)C_0^T(m_h^2) + 2\hat{t}(m_h^2 - \hat{t})C_0^T(\hat{t}) + 2\hat{u}(m_h^2 - \hat{u})C_0^T(\hat{u}) \right) \right\}. \end{aligned} \quad (15)$$

The top and T quark mixed contributions to f_B is given by $f_B^{tT} = (|y_L^{tT}|^2 + |y_R^{tT}|^2)f_B^{tT,\square 1} + [y_L^{tT}(y_R^{tT})^* + y_R^{tT}(y_L^{tT})^*]f_B^{tT,\square 2}$. Here, $f_B^{tT,\square 1}$ is defined as:

$$\begin{aligned} f_B^{tT,\square 1} = & \frac{2v^2}{\hat{s}} \left\{ -\frac{\hat{s}}{2} [C_0^t(\hat{s}) + C_0^T(\hat{s})] - \frac{1}{2} (\hat{s} - 2m_h^2 + 2m_t^2 + 2m_T^2) [C_0^{tT}(m_h^2) + C_0^{Tt}(m_h^2)] + \frac{m_h^2 - \hat{t}}{2} [C_0^{tT}(t) + C_0^{Tt}(t)] \right. \\ & + \frac{m_h^2 - \hat{u}}{2} [C_0^{tT}(u) + C_0^{Tt}(u)] + \frac{1}{2} (m_t^2 - m_T^2) (\hat{s} + m_t^2 + m_T^2 - m_h^2) [D_0^{tT}(\hat{t}, \hat{s}) + D_0^{tT}(\hat{u}, \hat{s}) - D_0^{Tt}(\hat{t}, \hat{s}) - D_0^{Tt}(\hat{u}, \hat{s})] \\ & + \frac{(m_t^2 + m_T^2)}{4} (\hat{s} - 2m_h^2 + 2m_t^2 + 2m_T^2) [D_0^{tT}(\hat{t}, \hat{s}) + D_0^{tT}(\hat{u}, \hat{s}) + D_0^{tT}(\hat{t}, \hat{u}) + D_0^{Tt}(\hat{t}, \hat{s}) + D_0^{Tt}(\hat{u}, \hat{s}) + D_0^{Tt}(\hat{t}, \hat{u})] \\ & + \frac{1}{4(\hat{t}\hat{u} - m_h^4)} [\hat{s}(\hat{s} - 2m_h^2)(\hat{s} - 2m_h^2 + 2m_t^2 + 2m_T^2) (C_0^t(\hat{s}) + C_0^T(\hat{s})) \\ & + 2\hat{s}(m_T^2 - m_t^2)(\hat{s} - 2m_h^2 + 2m_t^2 + 2m_T^2) (C_0^t(\hat{s}) - C_0^T(\hat{s})) + \hat{s}(\hat{s} - 4m_h^2)(\hat{s} - 2m_h^2 + 2m_t^2 + 2m_T^2) (C_0^{tT}(m_h^2) + C_0^{Tt}(m_h^2)) \\ & + 2\hat{t}(m_h^2 - \hat{t})(\hat{s} - 2m_h^2 + 2m_t^2 + 2m_T^2) (C_0^{tT}(\hat{t}) + C_0^{Tt}(\hat{t})) + 2\hat{u}(m_h^2 - \hat{u})(\hat{s} - 2m_h^2 + 2m_t^2 + 2m_T^2) (C_0^{tT}(\hat{u}) + C_0^{Tt}(\hat{u})) \\ & + \hat{s}(m_t^2 - m_T^2)^2 (\hat{s} - 2m_h^2 + 2m_t^2 + 2m_T^2) (D_0^{tT}(\hat{t}, \hat{s}) + D_0^{tT}(\hat{u}, \hat{s}) + D_0^{tT}(\hat{t}, \hat{u}) + D_0^{Tt}(\hat{t}, \hat{s}) + D_0^{Tt}(\hat{u}, \hat{s}) + D_0^{Tt}(\hat{t}, \hat{u})) \\ & + 2\hat{s}\hat{t}(m_t^2 - m_T^2)(\hat{s} - 2m_h^2 + 2m_t^2 + 2m_T^2) (D_0^{tT}(\hat{t}, \hat{s}) - D_0^{tT}(\hat{t}, \hat{s})) \\ & + 2\hat{s}\hat{u}(m_t^2 - m_T^2)(\hat{s} - 2m_h^2 + 2m_t^2 + 2m_T^2) (D_0^{tT}(\hat{u}, \hat{s}) - D_0^{tT}(\hat{u}, \hat{s})) \\ & - \hat{s}\hat{t}(\hat{t}^2 + m_h^4 - 2\hat{t}(m_t^2 + m_T^2)) (D_0^{tT}(\hat{t}, \hat{s}) + D_0^{tT}(\hat{u}, \hat{s})) - \hat{s}\hat{u}(\hat{u}^2 + m_h^4 - 2\hat{u}(m_t^2 + m_T^2)) (D_0^{Tt}(\hat{t}, \hat{s}) + D_0^{Tt}(\hat{u}, \hat{s})) \Big] \right\}, \end{aligned} \quad (16)$$

and $f_B^{tT,\square 2}$ is defined as

$$\begin{aligned} f_B^{tT,\square 2} = & \frac{2m_t m_T v^2}{\hat{s}} \left\{ -2 [C_0^{tT}(m_h^2) + C_0^{Tt}(m_h^2)] + 2m_t^2 [D_0^{tT}(\hat{t}, \hat{s}) + D_0^{tT}(\hat{u}, \hat{s}) + D_0^{tT}(\hat{t}, \hat{u})] \right. \\ & + 2m_T^2 [D_0^{Tt}(\hat{t}, \hat{s}) + D_0^{Tt}(\hat{u}, \hat{s}) + D_0^{Tt}(\hat{t}, \hat{u})] + \frac{1}{\hat{t}\hat{u} - m_h^4} [\hat{s}(\hat{s} - 2m_h^2) (C_0^t(\hat{s}) + C_0^T(\hat{s})) - 2\hat{s}(m_t^2 - m_T^2) (C_0^t(\hat{s}) - C_0^T(\hat{s})) \\ & + \hat{s}(\hat{s} - 4m_h^2) (C_0^{tT}(m_h^2) + C_0^{Tt}(m_h^2)) + 2\hat{t}(m_h^2 - \hat{t}) (C_0^{tT}(\hat{t}) + C_0^{Tt}(\hat{t})) + 2\hat{u}(m_h^2 - \hat{u}) (C_0^{tT}(\hat{u}) + C_0^{Tt}(\hat{u})) \\ & + \hat{s}(\hat{t}^2 + (m_t^2 - m_T^2)^2) (D_0^{tT}(\hat{t}, \hat{s}) + D_0^{tT}(\hat{t}, \hat{u})) + \hat{s}(\hat{u}^2 + (m_t^2 - m_T^2)^2) (D_0^{tT}(\hat{u}, \hat{s}) + D_0^{tT}(\hat{u}, \hat{u})) \\ & + 2\hat{s}\hat{t}(m_t^2 - m_T^2) (D_0^{tT}(\hat{t}, \hat{s}) - D_0^{tT}(\hat{t}, \hat{s})) + 2\hat{s}\hat{u}(m_t^2 - m_T^2) (D_0^{tT}(\hat{u}, \hat{s}) - D_0^{tT}(\hat{u}, \hat{s})) + 2\hat{s}(m_t^2 - m_T^2)^2 D_0^{tT}(\hat{t}, \hat{u}) \Big] \right\}. \end{aligned} \quad (17)$$

The pure top quark contribution to f_C is proportional to $\tilde{\kappa}_t$; hence, we set f_C^t to be zero. Similarly, the pure T quark contribution to f_C is also turned off. The top and T quark mixed contributions to f_C is given by $f_C^{tT} = -i[y_L^{tT}(y_R^{tT})^* - y_R^{tT}(y_L^{tT})^*]f_C^{tT,\square}$. Here, $f_C^{tT,\square}$ is defined as

$$\begin{aligned} f_C^{tT,\square} = & m_t m_T v^2 [D_0^{tT}(\hat{t}, \hat{s}) + D_0^{tT}(\hat{u}, \hat{s}) + D_0^{tT}(\hat{t}, \hat{u}) \\ & + D_0^{Tt}(\hat{t}, \hat{s}) + D_0^{Tt}(\hat{u}, \hat{s}) + D_0^{Tt}(\hat{t}, \hat{u})]. \end{aligned} \quad (18)$$

B. Heavy quark expansion

In the limit $\frac{m_h^2 \hat{s}, \hat{t}, \hat{u}}{m_t^2} \ll 1$, the coefficients of pure top quark loops f_A^t , f_B^t can be expanded as

$$\begin{aligned} f_A^{t,\triangle} = & \frac{2m_h^2}{\hat{s} - m_h^2} \left[1 + \frac{7\hat{s}}{120m_t^2} + O\left(\frac{1}{m_t^4}\right) \right], \\ f_A^{t,\square 1} = & -\frac{2}{3} \left[1 + \frac{7m_h^2}{20m_t^2} + O\left(\frac{1}{m_t^4}\right) \right], \\ f_B^{t,\square 1} = & \frac{11(m_h^4 - \hat{t}\hat{u})}{90m_t^2 \hat{s}} + O\left(\frac{1}{m_t^4}\right). \end{aligned} \quad (19)$$

Regarding the coefficients of pure T quark loops, they are just the ones with m_t replaced by m_T .

For the case of t and T quark mixed loops, there are

more complications. In the limit $\frac{m_h^2, \hat{s}, \hat{t}, \hat{u}}{m_{t,T}^2} \ll 1$, the coefficients f_A^{tT} , f_B^{tT} , f_C^{tT} can be expanded as

$$\begin{aligned} f_A^{tT,\square 1} &= \mathcal{O}\left(\frac{1}{m_{t,T}^4}\right), \quad f_A^{tT,\square 2} = -\frac{2v^2}{3m_t m_T} + \mathcal{O}\left(\frac{1}{m_{t,T}^4}\right), \\ f_C^{tT,\square} &= \frac{v^2}{m_t m_T} + \mathcal{O}\left(\frac{1}{m_{t,T}^4}\right), \\ f_B^{tT,\square 1} &= \frac{v^2(t^2 - \hat{u}^2)}{m_T^2(\hat{t}\hat{u} - m_h^4)} \cdot \frac{(1+r_{tT}^2)(1+2r_{tT}^2 \log r_{tT}^2 - r_{tT}^4)}{2r_{tT}^2(1-r_{tT}^2)^2} \\ &\quad + \mathcal{O}\left(\frac{1}{m_{t,T}^4}\right), \end{aligned}$$

$$f_B^{tT,\square 2} = \mathcal{O}\left(\frac{1}{m_{t,T}^4}\right). \quad (20)$$

In the above, r_{tT} is defined as $r_{tT} \equiv \frac{m_t}{m_T}$.

C. The cross section analysis

When averaging the initial spin and color degrees of freedom, we can obtain the partonic cross section of $gg \rightarrow hh$ at the leading order (LO) as follows:

$$\begin{aligned} \hat{\sigma}_{\text{LO}}(gg \rightarrow hh; \hat{s}) &= \frac{\alpha_s^2 G_F^2 \sqrt{\hat{s}(\hat{s}-4m_h^2)}}{128(4\pi)^3} \int_{-1}^1 d\cos\theta (|f_A|^2 + |f_B|^2 + |f_C|^2) \\ &= \frac{\alpha_s^2 G_F^2}{64(4\pi)^3} \int_{\hat{t}_{\min}}^{\hat{t}_{\max}} d\hat{t} (|f_A|^2 + |f_B|^2 + |f_C|^2) \left(\hat{t}_{\min} = -\frac{1}{4}(\sqrt{\hat{s}} + \sqrt{\hat{s}-4m_h^2})^2, \quad \hat{t}_{\max} = -\frac{1}{4}(\sqrt{\hat{s}} - \sqrt{\hat{s}-4m_h^2})^2 \right), \end{aligned} \quad (21)$$

where f_A, f_B, f_C are calculated as

$$\begin{aligned} f_A &= f_A^t + f_A^T + f_A^{tT} = \kappa_t f_A^{t,\triangle} + \kappa_t^2 f_A^{t,\square 1} + \left(-\frac{vy_T}{m_T}\right) f_A^{t,\triangle} + \left(\frac{vy_T}{m_T}\right)^2 f_A^{t,\square 1} + (|y_L^{tT}|^2 + |y_R^{tT}|^2) f_A^{t,\square 1} + [y_L^{tT}(y_R^{tT})^* + y_R^{tT}(y_L^{tT})^*] f_A^{t,\square 2}, \\ f_B &= f_B^t + f_B^T + f_B^{tT} = \kappa_t^2 f_B^{t,\square 1} + \left(\frac{vy_T}{m_T}\right)^2 f_B^{t,\square 1} + (|y_L^{tT}|^2 + |y_R^{tT}|^2) f_B^{t,\square 1} + [y_L^{tT}(y_R^{tT})^* + y_R^{tT}(y_L^{tT})^*] f_B^{t,\square 2}, \\ f_C &= f_C^t + f_C^T + f_C^{tT} = -i[y_L^{tT}(y_R^{tT})^* - y_R^{tT}(y_L^{tT})^*] f_C^{t,\square}. \end{aligned} \quad (22)$$

Note that there is a $\frac{1}{2}$ factor in the partonic cross section because of the identical final states. In general, the anomalous triple Higgs coupling λ_{hhh} will also alter the di-Higgs production cross section. Its effects can be captured with $f_A^{f,\triangle}, f_C^{f,\triangle} (f=t, T)$ multiplied by the factor $1 + \delta_{hhh} \equiv \lambda_{hhh}/\lambda_{hhh}^{SM}$.

After folding the partonic cross section with the gluon luminosity, we can get the hadron level cross section

$$\begin{aligned} \sigma_{\text{LO}}(pp \rightarrow hh) &= \int_{\frac{4m_h^2}{s}}^1 d\tau \int_{\tau}^1 \frac{dx}{x} f(x, \mu_F^2) \\ &\times f\left(\frac{\tau}{x}, \mu_F^2\right) \hat{\sigma}_{\text{LO}}(gg \rightarrow hh; \hat{s} = \tau s), \end{aligned} \quad (23)$$

where f represents the gluon parton distribution function (PDF) and μ_F is the factorization scale.

$$\begin{aligned} \mu_{hh} &= 1 + A_1 + A_0^{hhh} \delta_{hhh} + A_1^{hhh} \delta_{hhh}^2 + (A_2 + A_2^{hhh} \delta_{hhh})(|y_L^{tT}|^2 + |y_R^{tT}|^2) \\ &\quad + (A_3 + A_3^{hhh} \delta_{hhh})[y_L^{tT}(y_R^{tT})^* + y_R^{tT}(y_L^{tT})^*] + A_4(|y_L^{tT}|^2 + |y_R^{tT}|^2)^2 + A_5[y_L^{tT}(y_R^{tT})^* + y_R^{tT}(y_L^{tT})^*]^2 \\ &\quad + A_6(|y_L^{tT}|^2 + |y_R^{tT}|^2)[y_L^{tT}(y_R^{tT})^* + y_R^{tT}(y_L^{tT})^*] - A_7[y_L^{tT}(y_R^{tT})^* - y_R^{tT}(y_L^{tT})^*]^2, \end{aligned} \quad (25)$$

From the observation of Eqs. (21) and (22), we can

V. NUMERICAL RESULTS AND CONSTRAINT PROSPECTS

Similar to the VLQT model, for simplicity, we consider $\kappa_t = c_L^2, y_T = -\frac{m_T}{v} s_L^2$, but let $\text{Re}(y_L^{tT}), \text{Re}(y_R^{tT}), \text{Im}(y_L^{tT}), \text{Im}(y_R^{tT})$ to be free. Then we can select several benchmark scenarios and estimate the constraints on the magnitude and sign of the FCNY couplings. Now, we need to normalize the cross section to the SM ones numerically for fixed m_T and s_L , which is defined as

$$\mu_{hh} \equiv \frac{\sigma_{\text{LO}}(pp \rightarrow hh)}{\sigma_{\text{LO}}^{\text{SM}}(pp \rightarrow hh)}. \quad (24)$$

Up to LO level, μ_{hh} can be parametrized as

infer that $A_1, A_2, A_3, A_0^{hhh}, A_1^{hhh}, A_2^{hhh}, A_3^{hhh}$ depend on the

choices of both m_T and s_L , whereas A_4, A_5, A_6, A_7 solely depend on m_T . Moreover, A_1^{hhh}, A_4, A_5, A_7 are always non-negative, and A_1 vanishes as s_L tends to zero.

Although $\sigma^{\text{SM}}(pp \rightarrow hh)$ has been calculated with high precision [86-94], we will not consider this complex calculation here. Here, we only keep the LO results because a large part of the QCD corrections can be cancelled in the ratio [57, 65, 95, 96]. To obtain the numerical results of cross sections, we write a model file using FeynRules [97, 98], FeynArts [99], and NLOCT [100]. Then, this file is linked to MadGraph [101]. Before the numerical calculations, we use the following default settings:

- Proton contains b and \bar{b} , that is, we adopt the 5 flavor scheme.
- We adopt the PDF choice "MSTW2008lo68cl" (LHAPDF ID 21000 [102]).
- The default "*dynamical_scale_choice*" is set to be 3 (see [103]).
- The input parameters are selected as $m_h = 125.09 \text{ GeV}$, $G_F = 1.1664 \times 10^{-5} \text{ GeV}^{-2}$, $m_t = 172.74$

GeV, and $\alpha_s(m_Z) = 0.1184$; hence, $v = 246.221 \text{ GeV}$.

Currently, the Higgs pair production is bounded to be $|\mu_{hh}| \leq 6.9$ at 95% confidence level (CL) [104, 105]. At the high luminosity LHC (HL-LHC), di-Higgs production measurement is accessible. The expected signal strength is $\mu_{hh} = 1.00^{+0.41}_{-0.39}$ with 1σ uncertainty [106]. We set the benchmark points as $m_T = 400 \text{ GeV}$, $s_L = 0.2$ and $m_T = 800 \text{ GeV}$, $s_L = 0.1$, and the following discussions are based on the two benchmark points. Now, we should determine the specific values of $A_1, A_2, A_3, A_4, A_5, A_6, A_7$ and $A_0^{hhh}, A_1^{hhh}, A_2^{hhh}, A_3^{hhh}$. First, we have $\sigma_{\text{LO}}^{\text{SM}}(pp \rightarrow hh) = 24.7 \text{ fb}$. When setting different values of $\delta_{hhh}, y_L^{tT}, y_R^{tT}$, we can obtain different normalized cross sections (see Tables 1 and 2). Then, the numerical values of A_1, \dots, A_7 and $A_0^{hhh}, A_1^{hhh}, A_2^{hhh}, A_3^{hhh}$ can be solved from the first seven and last four equations separately. Their results are presented in Table 3.

A. Benchmark point $m_T = 400 \text{ GeV}$ and $s_L = 0.2$

For the case of $m_T = 400 \text{ GeV}$ and $s_L = 0.2$, the numerical results of μ_{hh} are evaluated as

$$\begin{aligned} \mu_{hh} = & 1 - 0.1919 - 0.6958 \delta_{hhh} + 0.2754 \delta_{hhh}^2 + (0.3717 - 0.1343 \delta_{hhh})(|y_L^{tT}|^2 + |y_R^{tT}|^2) \\ & + (1.672 - 0.9956 \delta_{hhh})[y_L^{tT}(y_R^{tT})^* + y_R^{tT}(y_L^{tT})^*] + 0.07449(|y_L^{tT}|^2 + |y_R^{tT}|^2)^2 + 1.114[y_L^{tT}(y_R^{tT})^* + y_R^{tT}(y_L^{tT})^*]^2 \\ & + 0.3166(|y_L^{tT}|^2 + |y_R^{tT}|^2)[y_L^{tT}(y_R^{tT})^* + y_R^{tT}(y_L^{tT})^*] - 3.071[y_L^{tT}(y_R^{tT})^* - y_R^{tT}(y_L^{tT})^*]^2. \end{aligned} \quad (26)$$

In this case, the present di-Higgs production experiments provide the constraints $\delta_{hhh} \in (-3.61, 6.13)$ and $\text{Re}y_L^{tT}, \text{Im}y_L^{tT}, \text{Re}y_R^{tT}, \text{Im}y_R^{tT} \in (-2.62, 2.62)$ at 95% CL by setting one parameter at a time. In Table 4, we provide the expected constraints on the parameters $\delta_{hhh}, \text{Re}y_L^{tT}, \text{Im}y_L^{tT}, \text{Re}y_R^{tT}, \text{Im}y_R^{tT}$ at HL-LHC. It can be observed that both the current and expected constraints at HL-LHC are stronger than the unitarity bound, because the highest power in di-

Higgs production cross section is proportional to $(y_{L,R}^{tT})^4$.

As mentioned above, there are four interesting parameters $\text{Re}(y_L^{tT}), \text{Re}(y_R^{tT}), \text{Im}(y_L^{tT}), \text{Im}(y_R^{tT})$. Accordingly, we can plot the reached two-dimensional parameter space by setting two of them to be zeros or imposing two conditions. Here, we select six scenarios: ① $y_{L,R}^{tT}$ are both real (similar to both imaginary number case); ② y_R^{tT} is real and y_L^{tT} is imaginary (similar to the real y_L^{tT} and imagin-

Table 1. Normalized cross sections for different $\delta_{hhh}, y_L^{tT}, y_R^{tT}$ values with $m_T = 400 \text{ GeV}$ and $s_L = 0.2$ at $\sqrt{s}=14 \text{ TeV}$.

δ_{hhh}	(y_L^{tT}, y_R^{tT})	expressions of μ_{hh}	numerical values of μ_{hh}
0	(0, 0)	$1 + A_1$	0.8081
	(0, 1)	$1 + A_1 + A_2 + A_4$	1.254
	(0, $\frac{1}{2}$)	$1 + A_1 + \frac{1}{4}A_2 + \frac{1}{16}A_4$	0.9057
	(1, 1)	$1 + A_1 + 2A_2 + 2A_3 + 4A_4 + 4A_5 + 4A_6$	10.92
	(1, -1)	$1 + A_1 + 2A_2 - 2A_3 + 4A_4 + 4A_5 - 4A_6$	1.695
	(1, i)	$1 + A_1 + 2A_2 + 4A_4 + 4A_7$	14.13
1	($\frac{1}{2}, \frac{1}{2}$)	$1 + A_1 + \frac{1}{2}A_2 + \frac{1}{2}A_3 + \frac{1}{4}A_4 + \frac{1}{4}A_5 + \frac{1}{4}A_6$	2.206
	(0, 0)	$1 + A_1 + A_0^{hhh} + A_1^{hhh}$	0.3877
	(0, 1)	$1 + A_1 + A_0^{hhh} + A_1^{hhh} + A_2 + A_2^{hhh} + A_4$	0.6996
-1	(1, 1)	$1 + A_1 + A_0^{hhh} + A_1^{hhh} + 2(A_2 + A_2^{hhh}) + 2(A_3 + A_3^{hhh}) + 4A_4 + 4A_5 + 4A_6$	8.235
	(0, 0)	$1 + A_1 - A_0^{hhh} + A_1^{hhh}$	1.779

Table 2. Normalized cross sections for different δ_{hhh} , y_L^{tT} , y_R^{tT} values with $m_T = 800$ GeV and $s_L = 0.1$ at $\sqrt{s}=14$ TeV.

δ_{hhh}	(y_L^{tT}, y_R^{tT})	expressions of μ_{hh}	numerical values of μ_{hh}
0	(0, 0)	$1 + A_1$	0.9506
	(0, 1)	$1 + A_1 + A_2 + A_4$	1.098
	(0, $\frac{1}{2}$)	$1 + A_1 + \frac{1}{4}A_2 + \frac{1}{16}A_4$	0.9838
	(1, 1)	$1 + A_1 + 2A_2 + 2A_3 + 4A_4 + 4A_5 + 4A_6$	5.255
	(1, -1)	$1 + A_1 + 2A_2 - 2A_3 + 4A_4 + 4A_5 - 4A_6$	0.3376
	(1, i)	$1 + A_1 + 2A_2 + 4A_4 + 4A_7$	5.247
	($\frac{1}{2}$, $\frac{1}{2}$)	$1 + A_1 + \frac{1}{2}A_2 + \frac{1}{2}A_3 + \frac{1}{4}A_4 + \frac{1}{4}A_5 + \frac{1}{4}A_6$	1.675
	(0, 0)	$1 + A_1 + A_0^{hhh} + A_1^{hhh}$	0.4502
1	(0, 1)	$1 + A_1 + A_0^{hhh} + A_1^{hhh} + A_2 + A_2^{hhh} + A_4$	0.5526
	(1, 1)	$1 + A_1 + A_0^{hhh} + A_1^{hhh} + 2(A_2 + A_2^{hhh}) + 2(A_3 + A_3^{hhh}) + 4A_4 + 4A_5 + 4A_6$	3.519
-1	(0, 0)	$1 + A_1 - A_0^{hhh} + A_1^{hhh}$	2.013

Table 3. Coefficients in Eq. (25) solved using the signal strength values in Tables 1 and 2.

\sqrt{s}/TeV	$(m_T/\text{GeV}, s_L)$	A_1	A_2	A_3	A_4	A_5	A_6	A_7
14	(400, 0.2)	-0.1919	0.3717	1.672	0.07449	1.114	0.3166	3.071
	(800, 0.1)	-0.04939	0.1279	1.087	0.01943	0.378	0.0711	0.9907
\sqrt{s}/TeV	$(m_T/\text{GeV}, s_L)$	A_0^{hhh}	A_1^{hhh}	A_2^{hhh}	A_3^{hhh}			
14	(400, 0.2)	-0.6958	0.2754	-0.1343	-0.9956			
	(800, 0.1)	-0.7814	0.281	-0.04494	-0.5731			

Table 4. Expected 1σ and 2σ bounds at HL-LHC for the parameters δ_{hhh} , $\text{Re}y_L^{tT}$, $\text{Im}y_L^{tT}$, $\text{Re}y_R^{tT}$, $\text{Im}y_R^{tT}$ under the benchmark point $m_T = 400$ GeV and $s_L = 0.2$. Here, we adopt two different methods: (1) turn on one parameter at a time (individual method) and (2) turn on all five parameters (marginalized method).

method	CL	δ_{hhh}	$\text{Re}y_L^{tT}$	$\text{Im}y_L^{tT}$	$\text{Re}y_R^{tT}$	$\text{Im}y_R^{tT}$
individual	1σ	(-0.681, 0.327) \cup (2.20, 3.21)	(-1.13, 1.13)	(-1.13, 1.13)	(-1.13, 1.13)	(-1.13, 1.13)
	2σ	(-1.03, 3.56)	(-1.40, 1.40)	(-1.40, 1.40)	(-1.40, 1.40)	(-1.40, 1.40)
marginalized	1σ	(-3.76, 3.99)	(-1.91, 1.91)	(-1.91, 1.91)	(-1.91, 1.91)	(-1.91, 1.91)
	2σ	(-4.48, 4.66)	(-2.09, 2.09)	(-2.09, 2.09)	(-2.09, 2.09)	(-2.09, 2.09)

ary y_R^{tT} case); ③ $y_R^{tT} = 0$ (similar to the $y_L^{tT} = 0$ case); ④ $y_L^{tT} = y_R^{tT}$; ⑤ $y_L^{tT} = -y_R^{tT}$; ⑥ $y_L^{tT} = (y_R^{tT})^*$.

In Figs. 5 and 6, we present the plots with $\delta_{hhh} = 0$ and $\delta_{hhh} = 0.5$, respectively. From these plots, we observe that $\text{Re}(y_{L,R}^{tT})$ and $\text{Im}(y_{L,R}^{tT})$ are constrained to be in the range $(-2, 2)$ approximately at 2σ CL. In some of these scenarios, the 2σ interval can be as tight as $(-0.4, 0.4)$. The reach regions of 1σ and 2σ are quite different. The value of δ_{hhh} has significant effects on the extraction of $y_{L,R}^{tT}$. For the first (upper left) plot, the first and third quadrants are more constrained. This can be understood from Eq. (22), because there is constructive interference between the positive $[y_L^{tT}(y_R^{tT})^* + y_R^{tT}(y_L^{tT})^*]$ term and other box diagram induced terms. However, it is a destructive interference if $[y_L^{tT}(y_R^{tT})^* + y_R^{tT}(y_L^{tT})^*]$ is negat-

ive. The last five plots are symmetric, relative to the horizontal and vertical axes. For the second (upper central) and sixth (lower right) plots, they receive contributions from the $[y_L^{tT}(y_R^{tT})^* - y_R^{tT}(y_L^{tT})^*]$ term. Because $|f_C|^2$ in Eq. (21) is always positive, the constraints are stronger. For the fourth (lower left) plot, positive $[y_L^{tT}(y_R^{tT})^* + y_R^{tT}(y_L^{tT})^*]$ induces the constructive interference; therefore, the bounds are also stronger. For the third (upper right) plot, both $[y_L^{tT}(y_R^{tT})^* + y_R^{tT}(y_L^{tT})^*]$ and $[y_L^{tT}(y_R^{tT})^* - y_R^{tT}(y_L^{tT})^*]$ vanish; hence, it is less constrained than other plots. In addition, there can be more cancellations between the triangle and box diagrams for larger δ_{hhh} . Therefore, the constraints are usually looser than the zero δ_{hhh} ones.

In fact, we infer that the di-Higgs production at HL-LHC can give stronger constraints than those from per-

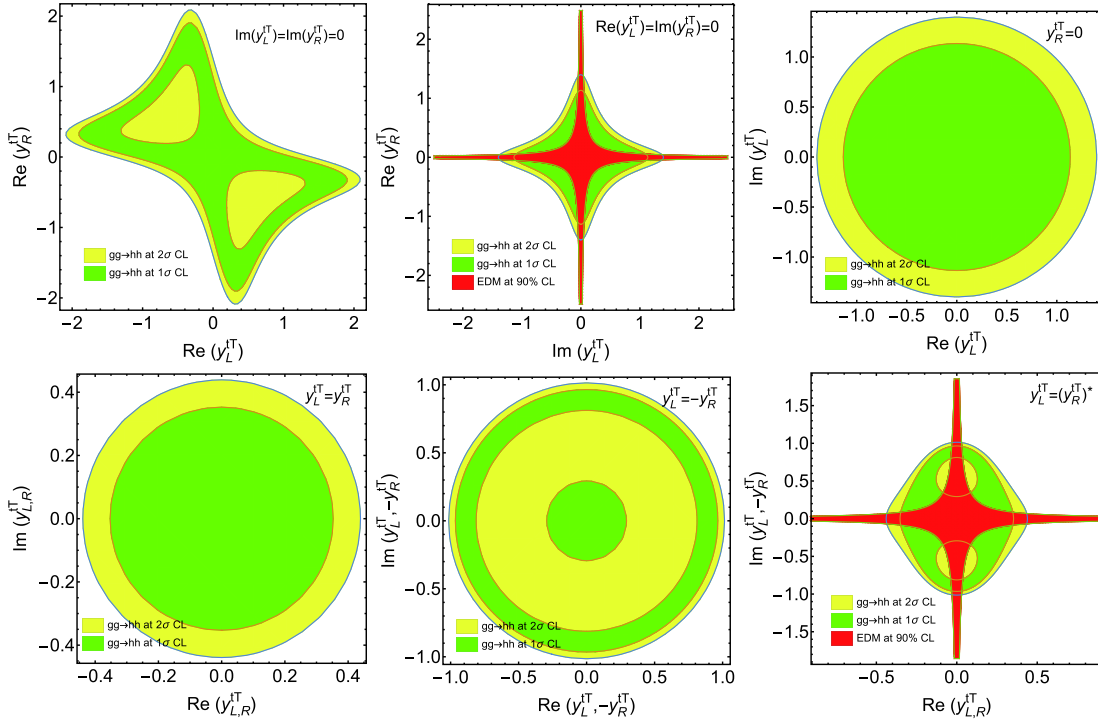


Fig. 5. (color online) Reach regions of y_L^{tT}, y_R^{tT} at HL-LHC with $\delta_{hhh} = 0$ for the case of $m_T = 400$ GeV and $s_L = 0.2$. In the above plots, we take $\text{Im}(y_L^{tT}) = \text{Im}(y_R^{tT}) = 0$ (upper left), $\text{Re}(y_L^{tT}) = \text{Im}(y_R^{tT}) = 0$ (upper central), $y_R^{tT} = 0$ (upper right), $y_L^{tT} = y_R^{tT}$ (lower left), $y_L^{tT} = -y_R^{tT}$ (lower central), and $y_L^{tT} = (y_R^{tT})^*$ (lower right). We also consider the top quark EDM constraint for the scenarios $\text{Re}(y_L^{tT}) = \text{Im}(y_R^{tT}) = 0$ (upper central) and $y_L^{tT} = (y_R^{tT})^*$ (lower right), where the reach regions of y_L^{tT}, y_R^{tT} are depicted in red at 90% CL.

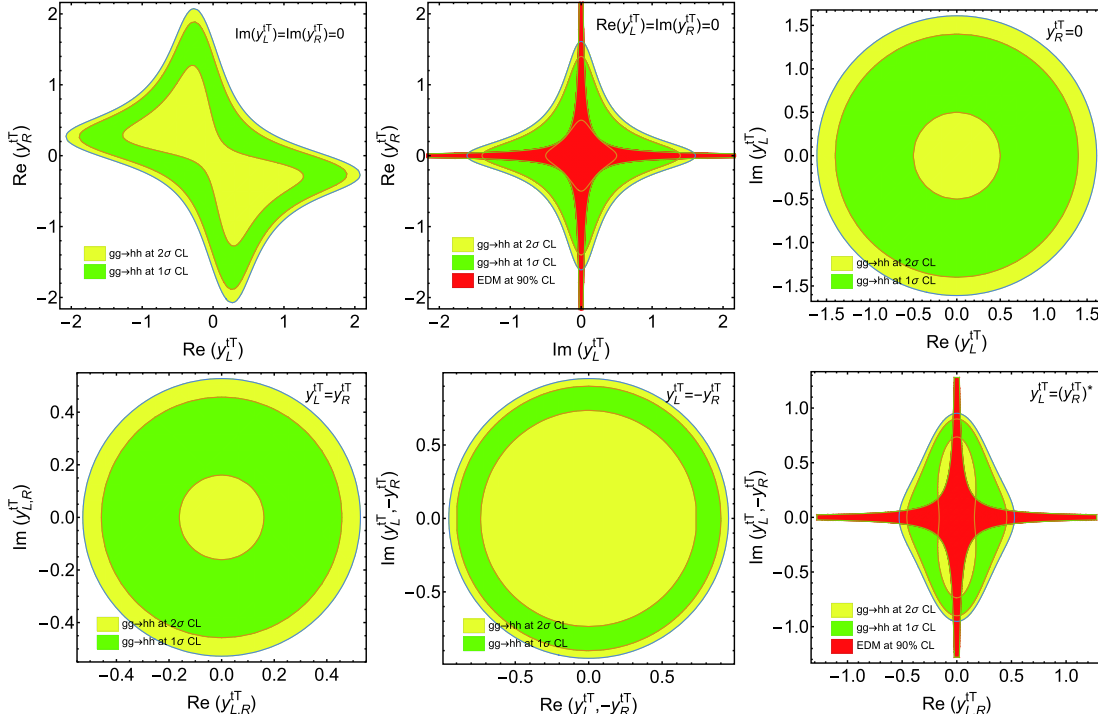


Fig. 6. (color online) Reach regions of y_L^{tT}, y_R^{tT} at HL-LHC with $\delta_{hhh} = 0.5$ for the case of $m_T = 400$ GeV and $s_L = 0.2$. In the above plots, we take $\text{Im}(y_L^{tT}) = \text{Im}(y_R^{tT}) = 0$ (upper left), $\text{Re}(y_L^{tT}) = \text{Im}(y_R^{tT}) = 0$ (upper central), $y_R^{tT} = 0$ (upper right), $y_L^{tT} = y_R^{tT}$ (lower left), $y_L^{tT} = -y_R^{tT}$ (lower central), and $y_L^{tT} = (y_R^{tT})^*$ (lower right). We also consider the top quark EDM constraint for the scenarios $\text{Re}(y_L^{tT}) = \text{Im}(y_R^{tT}) = 0$ (upper central) and $y_L^{tT} = (y_R^{tT})^*$ (lower right), where the reach regions of y_L^{tT}, y_R^{tT} are shown in red at 90% CL.

turbative unitarity and $h \rightarrow \gamma Z$ decay [17]. When we consider the top quark EDM bound, the two scenarios $\text{Re}(y_L^{tT}) = \text{Im}(y_R^{tT}) = 0$ and $y_L^{tT} = (y_R^{tT})^*$ can also be constrained. For the other scenarios $y_R^{tT} = 0, y_L^{tT} = \pm y_R^{tT}$, $\text{Im}y_L^{tT} = \text{Im}y_R^{tT} = 0$, they are insensitive to the top quark EDM, because we have the relationship $d_t^{\text{EDM}} \sim y_L^{tT}(y_L^{tT})^* - y_R^{tT}(y_R^{tT})^* = 2i(\text{Re}y_L^{tT}\text{Im}y_R^{tT} - \text{Re}y_R^{tT}\text{Im}y_L^{tT})$. For the scenarios $\text{Re}(y_L^{tT}) = \text{Im}(y_R^{tT}) = 0$ and $y_L^{tT} = (y_R^{tT})^*$, we compare the bounds from di-Higgs production and top quark EDM for

$$\begin{aligned} \mu_{hh} = & 1 - 0.04939 - 0.7814 \delta_{hhh} + 0.281 \delta_{hhh}^2 + (0.1279 - 0.04494 \delta_{hhh})(|y_L^{tT}|^2 + |y_R^{tT}|^2) \\ & + (1.087 - 0.5731 \delta_{hhh})[y_L^{tT}(y_R^{tT})^* + y_R^{tT}(y_L^{tT})^*] + 0.01943(|y_L^{tT}|^2 + |y_R^{tT}|^2)^2 + 0.378[y_L^{tT}(y_R^{tT})^* + y_R^{tT}(y_L^{tT})^*]^2 \\ & + 0.0711(|y_L^{tT}|^2 + |y_R^{tT}|^2)[y_L^{tT}(y_R^{tT})^* + y_R^{tT}(y_L^{tT})^*] - 0.9907[y_L^{tT}(y_R^{tT})^* - y_R^{tT}(y_L^{tT})^*]^2. \end{aligned} \quad (27)$$

In this case, the present di-Higgs production experiments give the constraints $\delta_{hhh} \in (-3.42, 6.20)$ and $\text{Re}y_L^{tT}, \text{Im}y_L^{tT}, \text{Re}y_R^{tT}, \text{Im}y_R^{tT} \in (-3.81, 3.81)$ at 95% CL by setting one parameter at a time. In Table 5, we provide the expected constraints on the parameters $\delta_{hhh}, \text{Re}y_L^{tT}, \text{Im}y_L^{tT}, \text{Re}y_R^{tT}, \text{Im}y_R^{tT}$ at HL-LHC.

We will also plot the reached two-dimensional parameter space by setting two of them to be zeros or imposing two conditions. In Figs. 7 and 8, similar plots are presented for the six scenarios with $\delta_{hhh} = 0$ and $\delta_{hhh} = 0.5$, respectively. From these plots, we infer that $\text{Re}(y_{L,R}^{tT})$ and $\text{Im}(y_{L,R}^{tT})$ are constrained to be in the range $(-3, 3)$ approximately at 2σ CL. In some of these scenarios, the 2σ interval can be as tight as $(-0.5, 0.5)$. The reach regions are similar to those in the $m_T = 400$ GeV and $s_L = 0.2$ case. Di-Higgs production at HL-LHC will give stronger constraints than those from $h \rightarrow \gamma Z$ decay under these scenarios [17]. For the scenarios $\text{Re}(y_L^{tT}) = \text{Im}(y_R^{tT}) = 0$ and $y_L^{tT} = (y_R^{tT})^*$, we also compare the bounds from di-Higgs production and top quark EDM for $\delta_{hhh} = 0$ (Fig. 7) and $\delta_{hhh} = 0.5$ (Fig. 8), respectively. When m_T becomes larger, $y_{L,R}^{tT}$ are constrained more loosely. When s_L becomes very small, the pure top quark contributions are SM-like, and the pure T quark contributions are highly suppressed. Therefore, the main deviation of μ_{hh} is from the FCNY interactions.

Table 5. Expected 1σ and 2σ bounds at HL-LHC for the parameters $\delta_{hhh}, \text{Re}y_L^{tT}, \text{Im}y_L^{tT}, \text{Re}y_R^{tT}, \text{Im}y_R^{tT}$ under the benchmark point $m_T = 800$ GeV and $s_L = 0.1$. Here, we adopt two different methods: (1) turn on one parameter at a time (individual method) and (2) turn on all five parameters (marginalized method).

method	CL	δ_{hhh}	$\text{Re}y_L^{tT}$	$\text{Im}y_L^{tT}$	$\text{Re}y_R^{tT}$	$\text{Im}y_R^{tT}$
individual	1σ	$(-0.499, 0.541) \cup (2.24, 3.28)$	$(-1.61, 1.61)$	$(-1.61, 1.61)$	$(-1.61, 1.61)$	$(-1.61, 1.61)$
	2σ	$(-0.852, 3.63)$	$(-2.04, 2.04)$	$(-2.04, 2.04)$	$(-2.04, 2.04)$	$(-2.04, 2.04)$
marginalized	1σ	$(-4.12, 3.89)$	$(-2.82, 2.82)$	$(-2.82, 2.82)$	$(-2.82, 2.82)$	$(-2.82, 2.82)$
	2σ	$(-4.80, 4.51)$	$(-3.05, 3.05)$	$(-3.05, 3.05)$	$(-3.05, 3.05)$	$(-3.05, 3.05)$

$\delta_{hhh} = 0$ (Fig. 5) and $\delta_{hhh} = 0.5$ (Fig. 6), respectively. From these plots, we can observe that the off-axis regions can be strongly bounded by the top EDM, whereas it will lose the constraining power in the near axis regions.

B. Benchmark point $m_T = 800$ GeV and $s_L = 0.1$

For the case of $m_T = 800$ GeV and $s_L = 0.1$, the numerical results of μ_{hh} are evaluated as:

By the way, the FCNY coupling may be probed via other processes too. For example, we can probe the FCNY coupling Tth via the direct production processes $pp \rightarrow T\bar{t}h, T\bar{t}h, ThW, Thj$. However, they are limited by low event rate, and the detailed analyses in these channels are beyond the scope of this work.

C. Comments on the doublet and triplet vector-like quarks

We have assumed $T_{L,R}$ to be singlets throughout this work, although they can be components of the doublet or triplet VLQs. There are two doublet and two triplet VLQs containing the T quark: $(X, T)_{L,R}, (T, B)_{L,R}, (X, T, B)_{L,R}, (T, B, Y)_{L,R}$. Here X, B, Y carry $\frac{4}{3}, -\frac{1}{3}, -\frac{4}{3}$ electric charges, respectively. For the doublet $(X, T)_{L,R}$, the Higgs particle solely interacts with the $T_{L,R}$. For the doublet $(T, B)_{L,R}$ and triplets $(X, T, B)_{L,R}, (T, B, Y)_{L,R}$, the B quark can mix with the SM bottom quark. Thus, the Higgs particle will interact with both the T and B quarks. Let us denote left (right) up-type and down-type quark mixing angles as θ_L^t (θ_R^t) and θ_L^b (θ_R^b), respectively. They can be related with each other [12].

- For the triplet $(X, T, B)_{L,R}$, we obtain the relationships $\tan\theta_R^t = \frac{m_t}{m_T} \tan\theta_L^t$ and $\tan\theta_R^b = \frac{m_b}{m_B} \tan\theta_L^b$. θ_L^t and θ_L^b

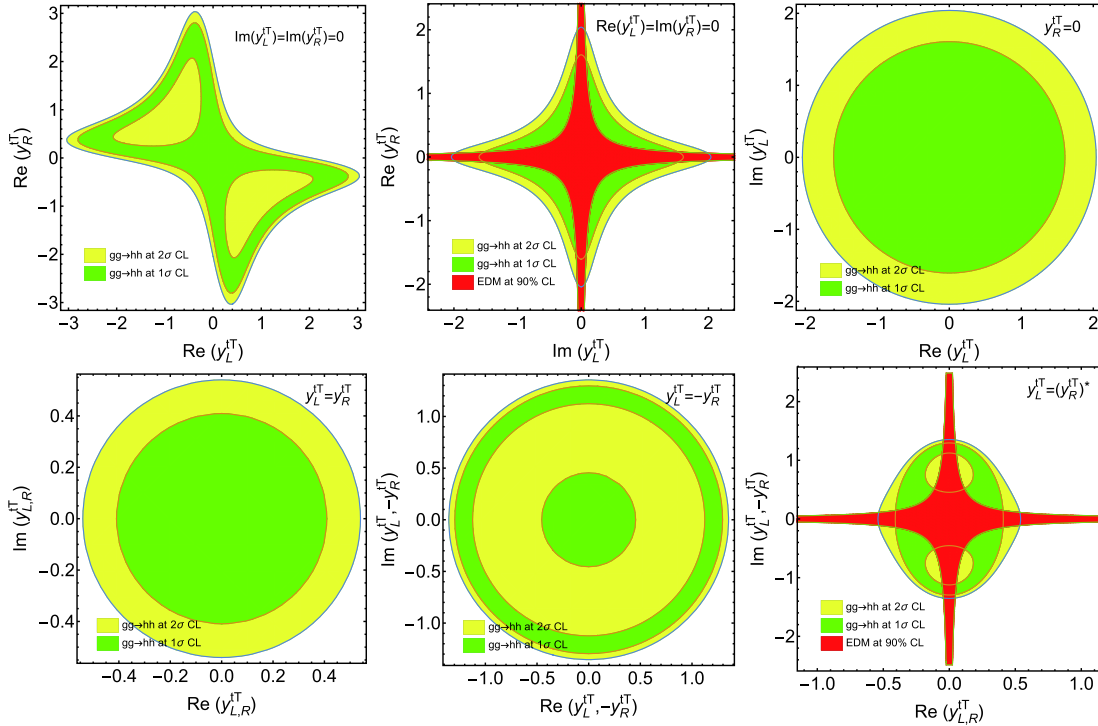


Fig. 7. (color online) Reach regions of y_L^{tT} , y_R^{tT} at HL-LHC with $\delta_{hhh} = 0$ for the case of $m_T = 800$ GeV and $s_L = 0.1$. In the above plots, we take $\text{Im}(y_L^{tT}) = \text{Im}(y_R^{tT}) = 0$ (upper left), $\text{Re}(y_L^{tT}) = \text{Im}(y_R^{tT}) = 0$ (upper central), $y_R^{tT} = 0$ (upper right), $y_L^{tT} = y_R^{tT}$ (lower left), $y_L^{tT} = -y_R^{tT}$ (lower central), and $y_L^{tT} = (y_R^{tT})^*$ (lower right). We also consider the top quark EDM constraint for the scenarios $\text{Re}(y_L^{tT}) = \text{Im}(y_R^{tT}) = 0$ (upper central) and $y_L^{tT} = (y_R^{tT})^*$ (lower right), where the reach regions of y_L^{tT} , y_R^{tT} are depicted in red at 90% CL.

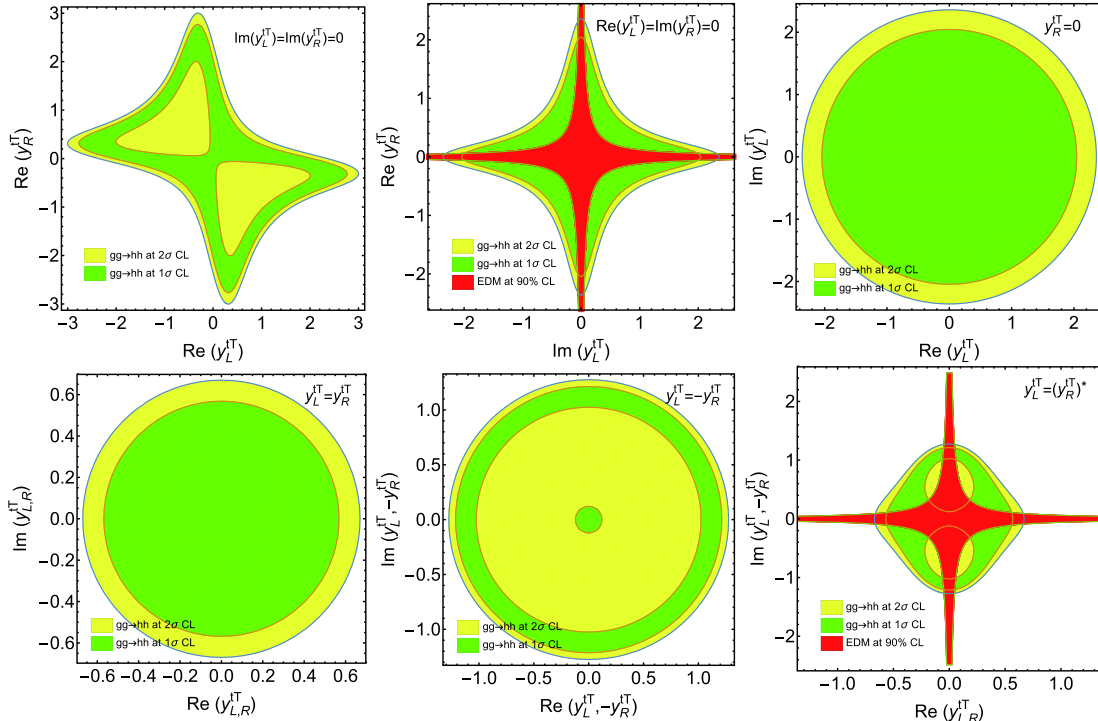


Fig. 8. (color online) Reach regions of y_L^{tT} , y_R^{tT} at HL-LHC with $\delta_{hhh} = 0.5$ for the case of $m_T = 800$ GeV and $s_L = 0.1$. In the above plots, we take $\text{Im}(y_L^{tT}) = \text{Im}(y_R^{tT}) = 0$ (upper left), $\text{Re}(y_L^{tT}) = \text{Im}(y_R^{tT}) = 0$ (upper central), $y_R^{tT} = 0$ (upper right), $y_L^{tT} = y_R^{tT}$ (lower left), $y_L^{tT} = -y_R^{tT}$ (lower central), and $y_L^{tT} = (y_R^{tT})^*$ (lower right). We also consider the top quark EDM constraint for the scenarios $\text{Re}(y_L^{tT}) = \text{Im}(y_R^{tT}) = 0$ (upper central) and $y_L^{tT} = (y_R^{tT})^*$ (lower right), where the reach regions of y_L^{tT} , y_R^{tT} are depicted in red at 90% CL.

can be related via the identity $\sin 2\theta_L^b = \sqrt{2} \frac{m_T^2 - m_t^2}{m_B^2 - m_b^2} \sin 2\theta_L^t$.

Thus, there is only one independent mixing angle θ_L^t .

- For the triplet $(T, B, Y)_{L,R}$, we have the relationships $\tan \theta_R^t = \frac{m_t}{m_T} \tan \theta_L^t$ and $\tan \theta_R^b = \frac{m_b}{m_B} \tan \theta_L^b$. θ_L^t and θ_L^b can be related via the identity

$\sin 2\theta_L^b = \frac{1}{\sqrt{2}} \frac{m_T^2 - m_t^2}{m_B^2 - m_b^2} \sin 2\theta_L^t$. Therefore, there is only one independent mixing angle θ_L^t .

- For the doublet $(X, T)_{L,R}$, we have the relationship $\tan \theta_L^t = \frac{m_t}{m_T} \tan \theta_R^t$. Thus, there is only one independent mixing angle θ_R^t .

- For the doublet $(T, B)_{L,R}$, we have the relationships $\tan \theta_L^t = \frac{m_t}{m_T} \tan \theta_R^t$ and $\tan \theta_L^b = \frac{m_b}{m_B} \tan \theta_R^b$. Hence, there are two independent mixing angles θ_R^t and θ_R^b .

For the doublet $(X, T)_{L,R}$, the constraints on FCNY couplings from di-Higgs production are similar to those in the singlet $T_{L,R}$ case. Compared to the singlet $T_{L,R}$, there are extra BBh, Bbh -type Yukawa interactions for the doublet $(T, B)_{L,R}$ and triplets $(X, T, B)_{L,R}, (T, B, Y)_{L,R}$. Therefore, the constraints on FCNY interactions are expected to be looser.

VI. SUMMARY AND CONCLUSIONS

Top partners are well motivated in many new physics models, and FCNY interactions can appear between top quark and the new heavy quark. To elucidate the nature of the flavor structure and EWSB, it is important to probe the FCNY interactions. However, it is challenging to directly constrain the Tth coupling at both current and future experiments.

In this study, we introduced a simplified model and summarized the main constraints from theoretical and experimental perspectives first. Then we calculated the amplitude of di-Higgs production. After selecting $m_T = 400$ GeV, $s_L = 0.2$ and $m_T = 800$ GeV, $s_L = 0.1$ as benchmark points, we evaluated the numerical cross sections. It is inferred that the present constraints from di-Higgs production have already surpassed the unitarity bound, owing to the $(y_{L,R}^{tT})^4$ behavior in di-Higgs production cross section. The constraints from di-Higgs production at HL-LHC are also stronger than the $h \rightarrow \gamma Z$ decay. For the case of $m_T = 400$ GeV and $s_L = 0.2$, $Re y_{L,R}^{tT}$ and $Im y_{L,R}^{tT}$ are expected to be bounded in the range $(-2, 2)$ and even $(-0.4, 0.4)$ in some scenarios at HL-LHC with 2σ CL approximately. For the case of $m_T = 800$ GeV and $s_L = 0.1$, $Re y_{L,R}^{tT}$ and $Im y_{L,R}^{tT}$ are expected to be bounded in the range $(-3, 3)$, and even $(-0.5, 0.5)$ in some scenarios at HL-LHC with 2σ CL approximately. The value of δ_{hhh} can have significant effects on the constraints of $y_{L,R}^{tT}$. In simple terms, larger δ_{hhh} values trigger looser constraints

on $y_{L,R}^{tT}$, as there can be more cancellations between the triangle and box diagrams. Finally, we determined that the top quark EDM can provide stronger bounds of $y_{L,R}^{tT}$ in the off-axis regions for some scenarios.

ACKNOWLEDGEMENTS

We would like to thank Gang Li, Zhao Li, Ying-nan Mao, and Hao Zhang for their helpful discussions. We also thank Olivier Mattelaer for MadGraph program discussions via the launchpad platform.

APPENDIX A: ASYMPTOTIC BEHAVIORS OF THE LOOP FUNCTIONS

1. The shorthand notations of C_0 and D_0 functions

The definitions of C_0 and D_0 functions related to pure top quark loops are given as

$$\begin{aligned} C'_0(\hat{s}) &\equiv C_0(0, 0, \hat{s}, m_t^2, m_t^2, m_t^2), \\ C'_0(m_h^2) &\equiv C_0(m_h^2, m_h^2, \hat{s}, m_t^2, m_t^2, m_t^2), \\ C'_0(\hat{t}) &\equiv C_0(0, m_h^2, \hat{t}, m_t^2, m_t^2, m_t^2), \\ C'_0(\hat{u}) &\equiv C_0(0, m_h^2, \hat{u}, m_t^2, m_t^2, m_t^2), \\ D'_0(\hat{t}, \hat{s}) &\equiv D_0(m_h^2, 0, 0, m_h^2, \hat{t}, \hat{s}, m_t^2, m_t^2, m_t^2), \\ D'_0(\hat{u}, \hat{s}) &\equiv D_0(m_h^2, 0, 0, m_h^2, \hat{u}, \hat{s}, m_t^2, m_t^2, m_t^2), \\ D'_0(\hat{t}, \hat{u}) &\equiv D_0(m_h^2, 0, m_h^2, 0, \hat{t}, \hat{u}, m_t^2, m_t^2, m_t^2, m_t^2). \end{aligned} \quad (A1)$$

The definitions of C_0 and D_0 functions related to pure T quark loops are given as

$$\begin{aligned} C_0^T(\hat{s}) &\equiv C_0(0, 0, \hat{s}, m_T^2, m_T^2, m_T^2), \\ C_0^T(m_h^2) &\equiv C_0(m_h^2, m_h^2, \hat{s}, m_T^2, m_T^2, m_T^2), \\ C_0^T(\hat{t}) &\equiv C_0(0, m_h^2, \hat{t}, m_T^2, m_T^2, m_T^2), \\ C_0^T(\hat{u}) &\equiv C_0(0, m_h^2, \hat{u}, m_T^2, m_T^2, m_T^2), \\ D_0^T(\hat{t}, \hat{s}) &\equiv D_0(m_h^2, 0, 0, m_h^2, \hat{t}, \hat{s}, m_T^2, m_T^2, m_T^2, m_T^2), \\ D_0^T(\hat{u}, \hat{s}) &\equiv D_0(m_h^2, 0, 0, m_h^2, \hat{u}, \hat{s}, m_T^2, m_T^2, m_T^2, m_T^2), \\ D_0^T(\hat{t}, \hat{u}) &\equiv D_0(m_h^2, 0, m_h^2, 0, \hat{t}, \hat{u}, m_T^2, m_T^2, m_T^2, m_T^2). \end{aligned} \quad (A2)$$

The definitions of C_0 and D_0 functions related to mixed t and T quark loops are given as

$$\begin{aligned} C_0^{tT}(m_h^2) &\equiv C_0(m_h^2, m_h^2, \hat{s}, m_t^2, m_T^2, m_t^2), \\ C_0^{tT}(\hat{t}) &\equiv C_0(0, m_h^2, \hat{t}, m_t^2, m_t^2, m_T^2), \\ C_0^{tT}(\hat{u}) &\equiv C_0(0, m_h^2, \hat{u}, m_t^2, m_t^2, m_T^2), \\ D_0^{tT}(\hat{t}, \hat{s}) &\equiv D_0(m_h^2, 0, 0, m_h^2, \hat{t}, \hat{s}, m_t^2, m_T^2, m_t^2, m_T^2), \\ D_0^{tT}(\hat{u}, \hat{s}) &\equiv D_0(m_h^2, 0, 0, m_h^2, \hat{u}, \hat{s}, m_t^2, m_t^2, m_T^2, m_T^2), \\ D_0^{tT}(\hat{t}, \hat{u}) &\equiv D_0(m_h^2, 0, m_h^2, 0, \hat{t}, \hat{u}, m_t^2, m_T^2, m_t^2, m_T^2), \end{aligned} \quad (A3)$$

and

$$\begin{aligned} C_0^{Tt}(m_h^2) &\equiv C_0(m_h^2, m_h^2, \hat{s}, m_T^2, m_t^2, m_T^2), \\ C_0^{Tt}(\hat{t}) &\equiv C_0(0, m_h^2, \hat{t}, m_T^2, m_T^2, m_t^2), \\ C_0^{Tt}(\hat{u}) &\equiv C_0(0, m_h^2, \hat{u}, m_T^2, m_T^2, m_t^2), \\ D_0^{Tt}(\hat{t}, \hat{s}) &\equiv D_0(m_h^2, 0, 0, m_h^2, \hat{t}, \hat{s}, m_t^2, m_T^2, m_T^2, m_T^2), \\ D_0^{Tt}(\hat{u}, \hat{s}) &\equiv D_0(m_h^2, 0, 0, m_h^2, \hat{u}, \hat{s}, m_t^2, m_T^2, m_T^2, m_T^2), \\ D_0^{Tt}(\hat{t}, \hat{u}) &\equiv D_0(m_h^2, 0, m_h^2, 0, \hat{t}, \hat{u}, m_T^2, m_t^2, m_t^2, m_T^2). \end{aligned} \quad (\text{A4})$$

In fact, we have the relationship $D_0^{Tt}(\hat{t}, \hat{u}) = D_0^{Tt}(\hat{t}, \hat{u})$.

2. Heavy quark expansion of C_0 function

C_0 function is defined as

$$\begin{aligned} C_0(k_1^2, k_{12}^2, k_2^2, m_0^2, m_1^2, m_2^2) \\ \equiv \frac{(2\pi\mu)^{4-D}}{i\pi^2} \int d^D q \frac{1}{(q^2 - m_0^2)[(q+k_1)^2 - m_1^2][(q+k_2)^2 - m_2^2]} \\ = - \int_0^1 \int_0^1 \int_0^1 dx dy dz \frac{\delta(x+y+z-1)}{xm_0^2 + ym_1^2 + zm_2^2 - xyk_1^2 - xzk_2^2 - yzk_{12}^2}, \end{aligned} \quad (\text{A5})$$

where $k_{12} \equiv k_1 - k_2$ and D is the dimension of space time. When the three internal masses are all equal, the C_0 function can be expanded as [86]

$$\begin{aligned} C_0(k_1^2, k_{12}^2, k_2^2, m_t^2, m_t^2, m_t^2) \\ = - \int_0^1 \int_0^1 \int_0^1 dx dy dz \frac{\delta(x+y+z-1)}{m_t^2 - xyk_1^2 - xzk_2^2 - yzk_{12}^2} \\ = - \frac{1}{2m_t^2} - \frac{k_1^2 + k_2^2 + k_{12}^2}{24m_t^4} - \frac{k_1^4 + k_2^4 + k_{12}^4 + k_1^2 k_2^2 + k_1^2 k_{12}^2 + k_2^2 k_{12}^2}{180m_t^6} \\ + O\left(\frac{k^6}{m_t^8}\right). \end{aligned} \quad (\text{A6})$$

In particular, we obtain the following results:

$$\begin{aligned} C_0^t(\hat{s}) &\approx -\frac{1}{2m_t^2} \left(1 + \frac{\hat{s}}{12m_t^2} + \frac{\hat{s}^2}{90m_t^4}\right), \\ C_0^t(m_h^2) &\approx -\frac{1}{2m_t^2} \left(1 + \frac{2m_h^2 + \hat{s}}{12m_t^2} + \frac{3m_h^4 + 2m_h^2 \hat{s} + \hat{s}^2}{90m_t^4}\right), \\ C_0^t(\hat{t}) &\approx -\frac{1}{2m_t^2} \left(1 + \frac{m_h^2 + \hat{t}}{12m_t^2} + \frac{m_h^4 + m_h^2 \hat{t} + \hat{t}^2}{90m_t^4}\right). \end{aligned} \quad (\text{A7})$$

The expansion of $C_0^t(\hat{u})$ functions can be obtained when replacing the \hat{t} in $C_0^t(\hat{t})$ with \hat{u} . The expansion of C_0^T functions can be obtained when replacing the m_t in C_0^t with m_T .

When the first two internal masses are equal, the C_0 function can be expanded as:

$$\begin{aligned} C_0(k_1^2, k_{12}^2, k_2^2, m_t^2, m_t^2, m_T^2) &= - \int_0^1 \int_0^1 \int_0^1 dx dy dz \frac{\delta(x+y+z-1)}{(x+y)m_t^2 + zm_T^2 - xyk_1^2 - xzk_2^2 - yzk_{12}^2} \\ &= - \int_0^1 \int_0^1 \int_0^1 dx dy dz \frac{\delta(x+y+z-1)}{(x+y)m_t^2 + zm_T^2} \left[1 + \frac{xyk_1^2 + xzk_2^2 + yzk_{12}^2}{(x+y)m_t^2 + zm_T^2} + \frac{(xyk_1^2 + xzk_2^2 + yzk_{12}^2)^2}{((x+y)m_t^2 + zm_T^2)^2}\right] + O\left(\frac{k^6}{m_{t,T}^8}\right) \\ &\approx \frac{1 + \log r_{iT}^2 - r_{iT}^2}{m_T^2(1 - r_{iT}^2)^2} - \frac{2 + 6r_{iT}^2 \log r_{iT}^2 + 3r_{iT}^2 - 6r_{iT}^4 + r_{iT}^6}{12m_T^4 r_{iT}^2 (1 - r_{iT}^2)^4} k_1^2 \\ &\quad + \frac{5 + 2(1 + 2r_{iT}^2) \log r_{iT}^2 - 4r_{iT}^2 - r_{iT}^4}{4m_T^4 (1 - r_{iT}^2)^4} (k_2^2 + k_{12}^2) \\ &\quad - \frac{3 - 30r_{iT}^2 - 20r_{iT}^4 (1 + 3 \log r_{iT}^2) + 60r_{iT}^6 - 15r_{iT}^8 + 2r_{iT}^{10}}{180m_T^6 r_{iT}^4 (1 - r_{iT}^2)^6} k_1^4 \\ &\quad + \frac{10 + 9r_{iT}^2 + 3(1 + 6r_{iT}^2 + 3r_{iT}^4) \log r_{iT}^2 - 18r_{iT}^4 - r_{iT}^6}{9m_T^6 (1 - r_{iT}^2)^6} (k_{12}^4 + k_2^2 k_{12}^2 + k_2^4) \\ &\quad - \frac{3 + 44r_{iT}^2 + 12r_{iT}^2 (2 + 3r_{iT}^2) \log r_{iT}^2 - 36r_{iT}^4 - 12r_{iT}^6 + r_{iT}^8}{36m_T^6 r_{iT}^2 (1 - r_{iT}^2)^6} k_1^2 (k_2^2 + k_{12}^2). \end{aligned} \quad (\text{A8})$$

When the first and third internal masses are equal, the C_0 function can be correlated with the first two mass equal cases via the following relationships:

$$\begin{aligned} C_0(k_1^2, k_{12}^2, k_2^2, m_t^2, m_T^2, m_t^2) &= C_0(k_2^2, k_{12}^2, k_1^2, m_t^2, m_t^2, m_T^2), \\ C_0(k_1^2, k_{12}^2, k_2^2, m_T^2, m_t^2, m_T^2) &= C_0(k_2^2, k_{12}^2, k_1^2, m_T^2, m_T^2, m_t^2). \end{aligned} \quad (\text{A9})$$

In particular, we obtain the following results:

$$\begin{aligned} C_0^{tT}(\hat{t}) &\approx \frac{1}{m_T^2} \cdot \frac{1 + \log r_{tT}^2 - r_{tT}^2}{(1 - r_{tT}^2)^2} + \frac{m_h^2 + \hat{t}}{m_T^4} \cdot \frac{5 + 2(1 + 2r_{tT}^2) \log r_{tT}^2 - 4r_{tT}^2 - r_{tT}^4}{4(1 - r_{tT}^2)^4} \\ &\quad + \frac{m_h^4 + m_h^2 \hat{t} + \hat{t}^2}{m_T^6} \cdot \frac{10 + 3(1 + 6r_{tT}^2 + 3r_{tT}^4) \log r_{tT}^2 + 9r_{tT}^2 - 18r_{tT}^4 - r_{tT}^6}{9(1 - r_{tT}^2)^6}, \\ C_0^{tT}(m_h^2) &\approx \frac{1}{m_T^2} \cdot \frac{1 + \log r_{tT}^2 - r_{tT}^2}{(1 - r_{tT}^2)^2} - \frac{\hat{s}}{m_T^4} \cdot \frac{2 + 6r_{tT}^2 \log r_{tT}^2 + 3r_{tT}^2 - 6r_{tT}^4 + r_{tT}^6}{12r_{tT}^2(1 - r_{tT}^2)^4} \\ &\quad + \frac{m_h^2}{m_T^4} \cdot \frac{5 + 2(1 + 2r_{tT}^2) \log r_{tT}^2 - 4r_{tT}^2 - r_{tT}^4}{2(1 - r_{tT}^2)^4} + \frac{m_h^4}{m_T^6} \cdot \frac{10 + 3(1 + 6r_{tT}^2 + 3r_{tT}^4) \log r_{tT}^2 + 9r_{tT}^2 - 18r_{tT}^4 - r_{tT}^6}{3(1 - r_{tT}^2)^6} \\ &\quad - \frac{m_h^2 \hat{s}}{m_T^6} \cdot \frac{3 + 12r_{tT}^2(2 + 3r_{tT}^2) \log r_{tT}^2 + 44r_{tT}^2 - 36r_{tT}^4 - 12r_{tT}^6 + r_{tT}^8}{18r_{tT}^2(1 - r_{tT}^2)^6} \\ &\quad - \frac{\hat{s}^2}{m_T^6} \cdot \frac{3 - 30r_{tT}^2 - 60r_{tT}^4 \log r_{tT}^2 - 20r_{tT}^4 + 60r_{tT}^6 - 15r_{tT}^8 + 2r_{tT}^{10}}{180r_{tT}^4(1 - r_{tT}^2)^6}. \end{aligned} \quad (\text{A10})$$

Maintaining the terms up to $\mathcal{O}\left(\frac{1}{m_T^4}\right)$, and considering the $\log r_{tT}^2$ -enhanced terms, they can be simplified as

$$\begin{aligned} C_0^{tT}(\hat{t}) &\approx \frac{1}{m_T^2} [1 + \log r_{tT}^2 + r_{tT}^2(1 + 2\log r_{tT}^2) + \frac{m_h^2 + \hat{t}}{4m_T^2}(5 + 2\log r_{tT}^2)], \\ C_0^{tT}(m_h^2) &\approx \frac{1}{m_T^2} [1 + \log r_{tT}^2 + r_{tT}^2(1 + 2\log r_{tT}^2) - \frac{\hat{s}}{12m_T^2} \left(\frac{2}{r_{tT}^2} + 11 + 6\log r_{tT}^2 \right) + \frac{m_h^2}{2m_T^2}(5 + 2\log r_{tT}^2)]. \end{aligned} \quad (\text{A11})$$

Similarly, we can obtain the following results

$$\begin{aligned} C_0^{Tt}(\hat{t}) &\approx -\frac{1}{m_T^2} \cdot \frac{1 + r_{tT}^2 \log r_{tT}^2 - r_{tT}^2}{(1 - r_{tT}^2)^2} - \frac{m_h^2 + \hat{t}}{m_T^4} \cdot \frac{1 + 2r_{tT}^2(2 + r_{tT}^2) \log r_{tT}^2 + 4r_{tT}^2 - 5r_{tT}^4}{4(1 - r_{tT}^2)^4} \\ &\quad - \frac{m_h^4 + m_h^2 \hat{t} + \hat{t}^2}{m_T^6} \cdot \frac{1 + 3r_{tT}^2(3 + 6r_{tT}^2 + r_{tT}^4) \log r_{tT}^2 + 18r_{tT}^2 - 9r_{tT}^4 - 10r_{tT}^6}{9(1 - r_{tT}^2)^6}, \\ C_0^{Tt}(m_h^2) &\approx -\frac{1}{m_T^2} \cdot \frac{1 + r_{tT}^2 \log r_{tT}^2 - r_{tT}^2}{(1 - r_{tT}^2)^2} - \frac{\hat{s}}{m_T^4} \cdot \frac{1 - 6r_{tT}^2 - 6r_{tT}^4 \log r_{tT}^2 + 3r_{tT}^4 + 2r_{tT}^6}{12(1 - r_{tT}^2)^4} \\ &\quad - \frac{m_h^2}{2m_T^4} \cdot \frac{1 + 2r_{tT}^2(2 + r_{tT}^2) \log r_{tT}^2 + 4r_{tT}^2 - 5r_{tT}^4}{(1 - r_{tT}^2)^4} - \frac{m_h^4}{m_T^6} \cdot \frac{1 + 3r_{tT}^2(3 + 6r_{tT}^2 + r_{tT}^4) \log r_{tT}^2 + 18r_{tT}^2 - 9r_{tT}^4 - 10r_{tT}^6}{3(1 - r_{tT}^2)^6} \\ &\quad - \frac{m_h^2 \hat{s}}{m_T^6} \cdot \frac{1 - 12r_{tT}^2 - 12r_{tT}^4(3 + 2r_{tT}^2) \log r_{tT}^2 - 36r_{tT}^4 + 44r_{tT}^6 + 3r_{tT}^8}{18(1 - r_{tT}^2)^6} \\ &\quad - \frac{\hat{s}^2}{m_T^6} \cdot \frac{2 - 15r_{tT}^2 + 60r_{tT}^4 + 60r_{tT}^6 \log r_{tT}^2 - 20r_{tT}^6 - 30r_{tT}^8 + 3r_{tT}^{10}}{180(1 - r_{tT}^2)^6}. \end{aligned} \quad (\text{A12})$$

Keeping the terms up to $\mathcal{O}\left(\frac{1}{m_T^4}\right)$, and considering the $\log r_{tT}^2$ -enhanced terms, they can be simplified as

$$C_0^{Tt}(\hat{t}) \approx -\frac{1}{m_T^2} \left[1 + r_{iT}^2(1 + \log r_{iT}^2) + \frac{m_h^2 + \hat{t}}{4m_T^2} \right], \quad C_0^{Tt}(m_h^2) \approx -\frac{1}{m_T^2} \left[1 + r_{iT}^2(1 + \log r_{iT}^2) + \frac{\hat{s}}{12m_T^2} + \frac{m_h^2}{2m_T^2} \right]. \quad (\text{A13})$$

3. Heavy quark expansion of D_0 function

D_0 function is defined as

$$\begin{aligned} D_0(k_1^2, k_{12}^2, k_{23}^2, k_3^2, k_2^2, k_{13}^2, m_0^2, m_1^2, m_2^2, m_3^2) \\ \equiv \frac{(2\pi\mu)^{4-D}}{i\pi^2} \int d^D q \frac{1}{(q^2 - m_0^2)[(q+k_1)^2 - m_1^2][(q+k_2)^2 - m_2^2][(q+k_3)^2 - m_3^2]} \\ = \int_0^1 \int_0^1 \int_0^1 \int_0^1 dx dy dz dw \frac{\delta(x+y+z+w-1)}{[xm_0^2 + ym_1^2 + zm_2^2 + wm_3^2 - xyk_1^2 - xzk_2^2 - xwk_3^2 - yzk_{12}^2 - ywk_{13}^2 - zwk_{23}^2]^2}, \end{aligned} \quad (\text{A14})$$

where $k_{12} \equiv k_1 - k_2$, $k_{23} \equiv k_2 - k_3$, and $k_{13} \equiv k_1 - k_3$. When the four internal masses are all equal, the D_0 function can be expanded as [86]

$$\begin{aligned} D_0(k_1^2, k_{12}^2, k_{23}^2, k_3^2, k_2^2, k_{13}^2, m_t^2, m_t^2, m_t^2, m_t^2) &= \int_0^1 \int_0^1 \int_0^1 \int_0^1 dx dy dz dw \frac{\delta(x+y+z+w-1)}{[m_t^2 - xyk_1^2 - xzk_2^2 - xwk_3^2 - yzk_{12}^2 - ywk_{13}^2 - zwk_{23}^2]^2} \\ &= \frac{1}{6m_t^4} \left[1 + \frac{k_1^2 + k_{12}^2 + k_{23}^2 + k_3^2 + k_2^2 + k_{13}^2}{10m_t^2} + \frac{1}{140m_t^4} (2(k_1^4 + k_2^4 + k_3^4 + k_1^2k_2^2 + k_1^2k_3^2 + k_2^2k_3^2) \right. \\ &\quad + 2(k_{12}^4 + k_{13}^4 + k_{23}^4 + k_{12}^2k_{13}^2 + k_{12}^2k_{23}^2 + k_{13}^2k_{23}^2) + 2k_1^2(k_{12}^2 + k_{13}^2) + 2k_2^2(k_{12}^2 + k_{23}^2) \\ &\quad \left. + 2k_3^2(k_{13}^2 + k_{23}^2) + (k_1^2k_{23}^2 + k_2^2k_{13}^2 + k_3^2k_{12}^2)) + O\left(\frac{k^6}{m_t^6}\right) \right]. \end{aligned} \quad (\text{A15})$$

In particular, we obtain the following results:

$$\begin{aligned} D_0^t(\hat{t}, \hat{s}) &\approx \frac{1}{6m_t^4} \left[1 + \frac{2m_h^2 + \hat{s} + \hat{t}}{10m_t^2} + \frac{6m_h^4 + 4m_h^2(\hat{s} + \hat{t}) + 2\hat{s}^2 + 2\hat{t}^2 + \hat{s}\hat{t}}{140m_t^4} \right], \\ D_0^t(\hat{t}, \hat{u}) &\approx \frac{1}{6m_t^4} \left[1 + \frac{2m_h^2 + \hat{t} + \hat{u}}{10m_t^2} + \frac{5m_h^4 + 4m_h^2(\hat{t} + \hat{u}) + 2\hat{t}^2 + 2\hat{u}^2 + \hat{t}\hat{u}}{140m_t^4} \right]. \end{aligned} \quad (\text{A16})$$

The expansion of $D_0^t(\hat{u}, \hat{s})$ can be obtained when replacing the \hat{t} in $D_0^t(\hat{t}, \hat{s})$ with \hat{u} . The expansion of D_0^T functions can be obtained when replacing the m_t in D_0^t with m_T .

When three internal masses are equal, the D_0 function can be expanded as

$$\begin{aligned} D_0(k_1^2, k_{12}^2, k_{23}^2, k_3^2, k_2^2, k_{13}^2, m_T^2, m_t^2, m_t^2, m_t^2) \\ = \int_0^1 \int_0^1 \int_0^1 \int_0^1 dx dy dz dw \frac{\delta(x+y+z+w-1)}{[xm_T^2 + (y+z+w)m_t^2 - xyk_1^2 - xzk_2^2 - xwk_3^2 - yzk_{12}^2 - ywk_{13}^2 - zwk_{23}^2]^2} \\ = \int_0^1 \int_0^1 \int_0^1 \int_0^1 dx dy dz dw \frac{\delta(x+y+z+w-1)}{[xm_T^2 + (y+z+w)m_t^2]^2} \left[1 + \frac{2(xy k_1^2 + xz k_2^2 + xw k_3^2 + yz k_{12}^2 + yw k_{13}^2 + zw k_{23}^2)}{xm_T^2 + (y+z+w)m_t^2} \right] + O\left(\frac{k^4}{m_{t,T}^8}\right) \\ \approx \frac{1}{m_T^4} \cdot \frac{1 + 2r_{iT}^2 \log r_{iT}^2 - r_{iT}^4}{2r_{iT}^2(1 - r_{iT}^2)^3} + \frac{(k_1^2 + k_2^2 + k_3^2)}{m_T^6} \cdot \frac{1 + 6r_{iT}^2(1 + r_{iT}^2) \log r_{iT}^2 + 9r_{iT}^2 - 9r_{iT}^4 - r_{iT}^6}{6r_{iT}^2(1 - r_{iT}^2)^5} \\ + \frac{(k_{12}^2 + k_{23}^2 + k_{13}^2)}{m_T^6} \cdot \frac{1 - 8r_{iT}^2 - 12r_{iT}^4 \log r_{iT}^2 + 8r_{iT}^6 - r_{iT}^8}{24r_{iT}^4(1 - r_{iT}^2)^5}. \end{aligned} \quad (\text{A17})$$

We only expand this equation up to $\mathcal{O}\left(\frac{k^2}{m_{t,T}^6}\right)$, because the general results will be relatively lengthy. For the integral $D_0^{TT}(\hat{t}, \hat{s})$, we obtain the expression up to $\mathcal{O}\left(\frac{k^4}{m_{t,T}^8}\right)$

$$\begin{aligned}
D_0^{TT}(\hat{t}, \hat{s}) &= \int_0^1 \int_0^1 \int_0^1 \int_0^1 dx dy dz dw \frac{\delta(x+y+z+w-1)}{[xm_T^2 + (y+z+w)m_t^2 - x(y+w)m_h^2 - xzt - yws]^2} \\
&= \int_0^1 \int_0^1 \int_0^1 \int_0^1 dx dy dz dw \frac{\delta(x+y+z+w-1)}{[xm_T^2 + (y+z+w)m_t^2]^2} \cdot \left(1 + \frac{2[x(y+w)m_h^2 + xzt + yws]}{xm_T^2 + (y+z+w)m_t^2} + \frac{3[x(y+w)m_h^2 + xzt + yws]^2}{[xm_T^2 + (y+z+w)m_t^2]^2}\right) \\
&\quad + \mathcal{O}\left(\frac{1}{m_{t,T}^{10}}\right) \approx \frac{1}{m_T^4} \cdot \frac{1+2r_{iT}^2 \log r_{iT}^2 - r_{iT}^4}{2r_{iT}^2(1-r_{iT}^2)^3} + \frac{(2m_h^2 + \hat{t})}{m_T^6} \cdot \frac{1+6r_{iT}^2(1+r_{iT}^2) \log r_{iT}^2 + 9r_{iT}^2 - 9r_{iT}^4 - r_{iT}^6}{6r_{iT}^2(1-r_{iT}^2)^5} \\
&\quad + \frac{\hat{s}}{m_T^6} \cdot \frac{1-8r_{iT}^2 - 12r_{iT}^4 \log r_{iT}^2 + 8r_{iT}^6 - r_{iT}^8}{24r_{iT}^4(1-r_{iT}^2)^5} + \frac{\hat{s}^2}{m_T^8} \cdot \frac{1-9r_{iT}^2 + 45r_{iT}^4 - 45r_{iT}^8 + 9r_{iT}^{10} - r_{iT}^{12} + 60r_{iT}^6 \log r_{iT}^2}{180r_{iT}^6(1-r_{iT}^2)^7} \\
&\quad + \frac{\hat{s}(\hat{t} + 4m_h^2)}{m_T^8} \cdot \frac{1-15r_{iT}^2 - 80r_{iT}^4 + 80r_{iT}^6 + 15r_{iT}^8 - r_{iT}^{10} - 60r_{iT}^4(1+r_{iT}^2) \log r_{iT}^2}{120r_{iT}^4(1-r_{iT}^2)^7} \\
&\quad + \frac{\hat{t}^2 + 2m_h^2\hat{t} + 3m_h^4}{m_T^8} \cdot \frac{1+28r_{iT}^2 - 28r_{iT}^6 - r_{iT}^8 + 12r_{iT}^2(1+3r_{iT}^2 + r_{iT}^4) \log r_{iT}^2}{12r_{iT}^2(1-r_{iT}^2)^7}.
\end{aligned} \tag{A18}$$

Keeping the terms up to $\mathcal{O}\left(\frac{1}{m_T^6}\right)$, and considering the $\log r_{iT}^2$ -enhanced terms, they can be simplified as

$$\begin{aligned}
D_0^{TT}(\hat{t}, \hat{s}) &\approx \frac{1}{2m_T^4} \left[\frac{1}{r_{iT}^2} + 3 + 2 \log r_{iT}^2 + r_{iT}^2(5 + 6 \log r_{iT}^2) \right] + \frac{(2m_h^2 + \hat{t})}{6m_T^6} \left(\frac{1}{r_{iT}^2} + 6 \log r_{iT}^2 + 14 \right) \\
&\quad + \frac{\hat{s}}{24m_T^6} \left(\frac{1}{r_{iT}^4} - \frac{3}{r_{iT}^2} - 12 \log r_{iT}^2 - 25 \right).
\end{aligned} \tag{A19}$$

Similarly, we can obtain the following results:

$$\begin{aligned}
D_0^{Tt}(\hat{t}, \hat{s}) &\approx \frac{1}{m_T^4} \cdot \frac{1+2r_{iT}^2 \log r_{iT}^2 - r_{iT}^4}{2(1-r_{iT}^2)^3} + \frac{(2m_h^2 + \hat{t})}{m_T^6} \cdot \frac{1+9r_{iT}^2 + 6r_{iT}^2(1+r_{iT}^2) \log r_{iT}^2 - 9r_{iT}^4 - r_{iT}^6}{6(1-r_{iT}^2)^5} \\
&\quad + \frac{\hat{s}}{m_T^6} \cdot \frac{1-8r_{iT}^2 - 12r_{iT}^4 \log r_{iT}^2 + 8r_{iT}^6 - r_{iT}^8}{24(1-r_{iT}^2)^5} + \frac{\hat{s}^2}{m_T^8} \cdot \frac{1-9r_{iT}^2 + 45r_{iT}^4 - 45r_{iT}^8 + 9r_{iT}^{10} - r_{iT}^{12} + 60r_{iT}^6 \log r_{iT}^2}{180(1-r_{iT}^2)^7} \\
&\quad + \frac{\hat{s}(\hat{t} + 4m_h^2)}{m_T^8} \cdot \frac{1-15r_{iT}^2 - 80r_{iT}^4 + 80r_{iT}^6 + 15r_{iT}^8 - r_{iT}^{10} - 60r_{iT}^4(1+r_{iT}^2) \log r_{iT}^2}{120(1-r_{iT}^2)^7} \\
&\quad + \frac{\hat{t}^2 + 2m_h^2\hat{t} + 3m_h^4}{m_T^8} \cdot \frac{1+28r_{iT}^2 - 28r_{iT}^6 - r_{iT}^8 + 12r_{iT}^2(1+3r_{iT}^2 + r_{iT}^4) \log r_{iT}^2}{12(1-r_{iT}^2)^7}.
\end{aligned} \tag{A20}$$

Keeping the terms up to $\mathcal{O}\left(\frac{1}{m_T^6}\right)$, and considering the $\log r_{iT}^2$ -enhanced terms, they can be simplified as:

$$D_0^{Tt}(\hat{t}, \hat{s}) \approx \frac{1}{2m_T^4} (1+3r_{iT}^2 + 2r_{iT}^2 \log r_{iT}^2) + \frac{2m_h^2 + \hat{t}}{6m_T^6} + \frac{\hat{s}}{24m_T^6}. \tag{A21}$$

When two internal masses are equal individually, we obtain the following relationships:

$$\begin{aligned} D_0(k_1^2, k_{12}^2, k_{23}^2, k_3^2, k_2^2, k_{13}^2, m_t^2, m_T^2, m_t^2) &= D_0(k_1^2, k_3^2, k_{23}^2, k_{12}^2, k_{13}^2, k_2^2, m_T^2, m_t^2, m_T^2) \\ &= D_0(k_{23}^2, k_3^2, k_1^2, k_{12}^2, k_2^2, k_{13}^2, m_T^2, m_t^2, m_T^2). \end{aligned} \quad (\text{A22})$$

D_0 function can be expanded as:

$$\begin{aligned} &D_0(k_1^2, k_{12}^2, k_{23}^2, k_3^2, k_2^2, k_{13}^2, m_T^2, m_t^2, m_T^2) \\ &= \int_0^1 \int_0^1 \int_0^1 \int_0^1 dx dy dz dw \frac{\delta(x+y+z+w-1)}{[(y+z)m_T^2 + (x+w)m_t^2 - xyk_1^2 - xzk_2^2 - xwk_3^2 - yzk_{12}^2 - ywk_{13}^2 - zwk_{23}^2]^2} \\ &= \int_0^1 \int_0^1 \int_0^1 \int_0^1 dx dy dz dw \frac{\delta(x+y+z+w-1)}{[(y+z)m_T^2 + (x+w)m_t^2]^2} \left[1 + \frac{2(xyk_1^2 + xzk_2^2 + xwk_3^2 + yzk_{12}^2 + ywk_{13}^2 + zwk_{23}^2)}{(y+z)m_T^2 + (x+w)m_t^2} \right] + O\left(\frac{k^4}{m_{t,T}^8}\right) \\ &\approx -\frac{1}{m_T^4} \cdot \frac{2 + (1+r_{tT}^2) \log r_{tT}^2 - 2r_{tT}^2}{(1-r_{tT}^2)^3} - \frac{k_1^2 + k_2^2 + k_{13}^2 + k_{23}^2}{m_T^6} \cdot \frac{3 + (1+4r_{tT}^2 + r_{tT}^4) \log r_{tT}^2 - 3r_{tT}^4}{2(1-r_{tT}^2)^5} \\ &\quad + \frac{k_3^2}{m_T^6} \cdot \frac{1 + 6r_{tT}^2(1+r_{tT}^2) \log r_{tT}^2 + 9r_{tT}^2 - 9r_{tT}^4 - r_{tT}^6}{6r_{tT}^2(1-r_{tT}^2)^5} + \frac{k_{12}^2}{m_T^6} \cdot \frac{1 + 6r_{tT}^2(1+r_{tT}^2) \log r_{tT}^2 + 9r_{tT}^2 - 9r_{tT}^4 - r_{tT}^6}{6(1-r_{tT}^2)^5}. \end{aligned} \quad (\text{A23})$$

We only expand it up to $O\left(\frac{k^2}{m_{t,T}^6}\right)$, because the general results will be relatively lengthy. For the integral $D_0^{tT}(\hat{t}, \hat{u})$, we obtain the expression up to $O\left(\frac{k^4}{m_{t,T}^8}\right)$

$$\begin{aligned} D_0^{tT}(\hat{t}, \hat{u}) &= \int_0^1 \int_0^1 \int_0^1 \int_0^1 dx dy dz dw \frac{\delta(x+y+z+w-1)}{[(x+w)m_t^2 + (y+z)m_T^2 - (xy + zw)m_h^2 - xzt - ywu]^2} \\ &= \int_0^1 \int_0^1 \int_0^1 \int_0^1 dx dy dz dw \frac{\delta(x+y+z+w-1)}{[(x+w)m_t^2 + (y+z)m_T^2]^2} \cdot \\ &\quad \left(1 + \frac{2[(xy + zw)m_h^2 + xzt + ywu]}{(x+w)m_t^2 + (y+z)m_T^2} + \frac{3[(xy + zw)m_h^2 + xzt + ywu]^2}{[(x+w)m_t^2 + (y+z)m_T^2]^2} \right) + O\left(\frac{1}{m_{t,T}^{10}}\right) \\ &\approx -\frac{1}{m_T^4} \cdot \frac{2 + (1+r_{tT}^2) \log r_{tT}^2 - 2r_{tT}^2}{(1-r_{tT}^2)^3} - \frac{2m_h^2 + \hat{t} + \hat{u}}{m_T^6} \cdot \frac{3 + (1+4r_{tT}^2 + r_{tT}^4) \log r_{tT}^2 - 3r_{tT}^4}{2(1-r_{tT}^2)^5} \\ &\quad - \frac{5m_h^4 + 4m_h^2(\hat{t} + \hat{u}) + 2\hat{t}^2 + \hat{t}\hat{u} + 2\hat{u}^2}{m_T^8} \cdot \frac{11 + 27r_{tT}^2 - 27r_{tT}^4 - 11r_{tT}^6 + 3(1+9r_{tT}^2 + 9r_{tT}^4 + r_{tT}^6) \log r_{tT}^2}{18(1-r_{tT}^2)^7}. \end{aligned} \quad (\text{A24})$$

Keeping the terms up to $O\left(\frac{1}{m_T^4}\right)$, and considering the $\log r_{tT}^2$ enhanced terms, they can be simplified as

$$D_0^{tT}(\hat{t}, \hat{u}) \approx -\frac{1}{m_T^4} \left[2 + \log r_{tT}^2 + 4r_{tT}^2(1 + \log r_{tT}^2) \right] - \frac{4m_h^2 - \hat{s}}{2m_T^6} (3 + \log r_{tT}^2). \quad (\text{A25})$$

In the above calculations, the t and T quark mixed C_0 and D_0 integrals will agree with the pure top quark integrals in the limit of $m_t = m_T$ (or $r_{tT} \rightarrow 1$). In addition, these

expansion results have been numerically verified by LoopTools [107].

References

- [1] S. L. Glashow, *Nucl. Phys.* **22**, 579-588 (1961)
- [2] Steven Weinberg, *Phys. Rev. Lett.* **19**, 1264-1266 (1967)

- [3] Abdus Salam, *Conf. Proc. C* **680519**, 367-377 (1968)
- [4] M. Tanabashi *et al.*, *Phys. Rev. D* **98**(3), 030001 (2018)
- [5] F. Englert and R. Brout, *Phys. Rev. Lett.* **13**, 321-323 (1964)

- [6] Peter W. Higgs, Phys. Lett. **12**, 132-133 (1964)
- [7] G. S. Guralnik, C. R. Hagen, and T. W. B. Kibble, Phys. Rev. Lett. **13**, 585-587 (1964)
- [8] T. W. B. Kibble, Phys. Rev. **155**, 1554-1561 (1967)
- [9] Georges Aad *et al.*, Phys. Lett. B **716**, 1-29 (2012)
- [10] Serguei Chatrchyan *et al.*, Phys. Lett. B **716**, 30-61 (2012)
- [11] J. A. Aguilar-Saavedra, JHEP **11**, 030 (2009)
- [12] J. A. Aguilar-Saavedra, R. Benbrik, S. Heinemeyer *et al.*, Phys. Rev. D **88**(9), 094010 (2013)
- [13] S. Dittmaier *et al.*, *Handbook of LHC Higgs Cross Sections: 1. Inclusive Observables*. 2011
- [14] S. Dittmaier *et al.*, *Handbook of LHC Higgs Cross Sections: 2. Differential Distributions*. 2012
- [15] J. R. Andersen *et al.*, *Handbook of LHC Higgs Cross Sections: 3. Higgs Properties*. 2013
- [16] D. de Florian *et al.*, *Handbook of LHC Higgs Cross Sections: 4. Deciphering the Nature of the Higgs Sector*. 2016
- [17] Shi-Ping He, Phys. Rev. D **102**(7), 075035 (2020)
- [18] S. Dawson and E. Furlan, Phys. Rev. D **86**, 015021 (2012)
- [19] Andrea De Simone, Oleksii Matsedonskyi, Riccardo Rattazzi *et al.*, JHEP **04**, 004 (2013)
- [20] F. del Aguila, M. Perez-Victoria, and Jose Santiago, Phys. Lett. B **492**, 98-106 (2000)
- [21] F. del Aguila, M. Perez-Victoria, and Jose Santiago, JHEP **09**, 011 (2000)
- [22] J. A. Aguilar-Saavedra, Phys. Rev. D **67**, 035003 (2003) [Erratum: Phys. Rev. D **69**, 099901 (2004)]
- [23] Matthew J. Dolan, J. L. Hewett, M. Krämer *et al.*, JHEP **07**, 039 (2016)
- [24] Jeong Han Kim and Ian M. Lewis, JHEP **05**, 095 (2018)
- [25] J. A. Aguilar-Saavedra, D. E. López-Fogliani, and C. Muñoz, JHEP **06**, 095 (2017)
- [26] Margarete Mühlleitner, Marco O. P. Sampaio, Rui Santos *et al.*, JHEP **03**, 094 (2017)
- [27] Kingman Cheung, Shi-Ping He, Ying-nan Mao *et al.*, Phys. Rev. D **98**(7), 075023 (2018)
- [28] Giacomo Cacciapaglia, Thomas Flacke, Myeonghun Park *et al.*, Phys. Lett. B **798**, 135015 (2019)
- [29] Mathieu Buchkremer, Giacomo Cacciapaglia, Aldo Deandrea *et al.*, Nucl. Phys. B **876**, 376-417 (2013)
- [30] Shinya Kanemura, Yasuhiro Okada, Eibun Senaha *et al.*, Phys. Rev. D **70**, 115002 (2004)
- [31] Shi-Ping He and Shou-hua Zhu, Phys. Lett. B, **764**, 31-37 (2017). [Erratum: Phys. Lett. B **797**, 134782 (2019)]
- [32] Shinya Kanemura, Mariko Kikuchi, and Kei Yagyu, Nucl. Phys. B **917**, 154-177 (2017)
- [33] Abdesslam Arhrib, Rachid Benbrik, Jaouad El Falaki *et al.*, JHEP **12**, 007 (2015)
- [34] Shinya Kanemura, Mariko Kikuchi, Kodai Sakurai *et al.*, Comput. Phys. Commun. **233**, 134-144 (2018)
- [35] Cheng-Wei Chiang, An-Li Kuo, and Kei Yagyu, Phys. Rev. D **98**(1), 013008 (2018)
- [36] Johannes Braathen and Shinya Kanemura, Phys. Lett. B **796**, 38-46 (2019)
- [37] Christoph Englert and Joerg Jaeckel, Phys. Rev. D **100**(9), 095017 (2019)
- [38] Shinya Kanemura, Mariko Kikuchi, Kentarou Mawatari *et al.*, Comput. Phys. Commun. **257**, 107512 (2020)
- [39] Christoph Englert, Joerg Jaeckel, Michael Spannowsky *et al.*, Phys. Lett. B **806**, 135526 (2020)
- [40] Michael E. Peskin and Tatsu Takeuchi, Phys. Rev. Lett. **65**, 964-967 (1990)
- [41] Michael E. Peskin and Tatsu Takeuchi, Phys. Rev. D **46**, 381-409 (1992)
- [42] L. Lavoura and Joao P. Silva, Phys. Rev. D **47**, 2046-2057 (1993)
- [43] Chien-Yi Chen, S. Dawson, and Elisabetta Furlan, Phys. Rev. D **96**(1), 015006 (2017)
- [44] Jernej F. Kamenik, Michele Papucci, and Andreas Weiler, Phys. Rev. D **85**, 071501 (2012) [Erratum: Phys. Rev. D **88**, 039903 (2013)]
- [45] V. Cirigliano, W. Dekens, J. de Vries *et al.*, Phys. Rev. D **94**(1), 016002 (2016)
- [46] V. Cirigliano, W. Dekens, J. de Vries *et al.*, Phys. Rev. D **94**(3), 034031 (2016)
- [47] Jacob Baron *et al.*, Science **343**, 269-272 (2014)
- [48] V. Andreev *et al.*, Nature **562**(7727), 355-360 (2018)
- [49] E. W. Nigel Glover and J. J. van der Bij, Nucl. Phys. B **309**, 282-294 (1988)
- [50] Abdelhak Djouadi, Phys. Rept. **457**, 1-216 (2008)
- [51] Eri Asakawa, Daisuke Harada, Shinya Kanemura *et al.*, Phys. Rev. D **82**, 115002 (2010)
- [52] Matthew J. Dolan, Christoph Englert, and Michael Spannowsky, Phys. Rev. D **87**(5), 055002 (2013)
- [53] S. Dawson, A. Ismail, and Ian Low, Phys. Rev. D **91**(11), 115008 (2015)
- [54] Hong-Jian He, Jing Ren, and Weiming Yao, Phys. Rev. D **93**(1), 015003 (2016)
- [55] J. Alison *et al.*, Higgs Boson Pair Production at Colliders: Status and Perspectives. In B. Di Micco, M. Gouzevitch, J. Mazzitelli, and C. Vernieri, editors, *Double Higgs Production at Colliders*, 9 2019
- [56] Florian Goertz, Andreas Papaefstathiou, Li Lin Yang *et al.*, JHEP **04**, 167 (2015)
- [57] Aleksandr Azatov, Roberto Contino, Giuliano Panico *et al.*, Phys. Rev. D **92**(3), 035001 (2015)
- [58] Chih-Ting Lu, Jung Chang, Kingman Cheung *et al.*, JHEP **08**, 133 (2015)
- [59] Qing-Hong Cao, Bin Yan, Dong-Ming Zhang *et al.*, Phys. Lett. B **752**, 285-290 (2016)
- [60] Qing-Hong Cao, Gang Li, Bin Yan *et al.*, Phys. Rev. D **96**(9), 095031 (2017)
- [61] Gang Li, Ling-Xiao Xu, Bin Yan *et al.*, Phys. Lett. B **800**, 135070 (2020)
- [62] Roberto Contino, Christophe Grojean, Mauro Moretti *et al.*, JHEP **05**, 089 (2010)
- [63] Roberto Contino, Margherita Ghezzi, Mauro Moretti *et al.*, JHEP **08**, 154 (2012)
- [64] R. Grober, M. Mühlleitner, and M. Spira, Nucl. Phys. B **925**, 1-27 (2017)
- [65] G. Buchalla, M. Capozzi, A. Celis *et al.*, JHEP **09**, 057 (2018)
- [66] Chien-Yi Chen, S. Dawson, and I. M. Lewis, Phys. Rev. D **91**(3), 035015 (2015)
- [67] S. Dawson and I. M. Lewis, Phys. Rev. D **92**(9), 094023 (2015)
- [68] Ian M. Lewis and Matthew Sullivan, Phys. Rev. D **96**(3), 035037 (2017)
- [69] Lan-Chun Lü, Chun Du, Yaquan Fang *et al.*, Phys. Lett. B **755**, 509-522 (2016)
- [70] Stefania De Curtis, Stefano Moretti, Kei Yagyu *et al.*, Phys. Rev. D **95**(9), 095026 (2017)
- [71] Tadashi Kon, Takuto Nagura, Takahiro Ueda *et al.*, Phys. Rev. D **99**(9), 095027 (2019)
- [72] Jing Ren, Rui-Qing Xiao, Maosen Zhou *et al.*, JHEP **06**,

- 090 (2018)
- [73] Sally Dawson, Elisabetta Furlan, and Ian Lewis, [Phys. Rev. D](#) **87**(1), 014007 (2013)
- [74] Giacomo Cacciapaglia, Haiying Cai, Alexandra Carvalho *et al.*, [JHEP](#) **07**, 005 (2017)
- [75] Kingman Cheung, Adil Jueid, Chih-Ting Lu *et al.*, *Disentangling new physics effects on non-resonant Higgs boson pair production from gluon fusion. 3* (2020)
- [76] M. Gillioz, R. Grober, C. Grojean *et al.*, [JHEP](#) **10**, 004 (2012)
- [77] Ramona Grober, Margarete Muhlleitner, and Michael Spira, [JHEP](#) **06**, 080 (2016)
- [78] T. Plehn, M. Spira, and P.M. Zerwas, [Nucl. Phys. B](#) **479**, 46-64 (1996) [Erratum: [Nucl. Phys. B](#) **531**, 655-655 (1998)]
- [79] S. Dawson, S. Dittmaier, and M. Spira, [Phys. Rev. D](#) **58**, 115012 (1998)
- [80] Abdelhak Djouadi, [Phys. Rept.](#) **459**, 1-241 (2008)
- [81] Junjie Cao, Zhaoxia Heng, Liangliang Shang *et al.*, [JHEP](#) **04**, 134 (2013)
- [82] Philipp Basler, Sally Dawson, Christoph Englert *et al.*, [Phys. Rev. D](#) **99**(5), 055048 (2019)
- [83] D. Binosi, J. Collins, C. Kaufhold *et al.*, [Comput. Phys. Commun.](#) **180**, 1709-1715 (2009)
- [84] R. Mertig, M. Bohm, and Ansgar Denner, [Comput. Phys. Commun.](#) **64**, 345-359 (1991)
- [85] Vladyslav Shtabovenko, Rolf Mertig, and Frederik Orellana, [Comput. Phys. Commun.](#) **207**, 432-444 (2016)
- [86] Ding Yu Shao, Chong Sheng Li, Hai Tao Li *et al.*, [JHEP](#) **07**, 169 (2013)
- [87] Daniel de Florian and Javier Mazzitelli, [Phys. Rev. Lett.](#) **111**, 201801 (2013)
- [88] Daniel de Florian and Javier Mazzitelli, [JHEP](#) **09**, 053 (2015)
- [89] Giuseppe Degrassi, Pier Paolo Giardino, and Ramona Gröber, [Eur. Phys. J. C](#) **76**(7), 411 (2016)
- [90] S. Borowka, N. Greiner, G. Heinrich *et al.*, [Phys. Rev. Lett.](#) **117**(1), 012001 (2016) [Erratum: [Phys. Rev. Lett.](#) **117**, 079901 (2016)]
- [91] Massimiliano Grazzini, Gudrun Heinrich, Stephen Jones *et al.*, [JHEP](#) **05**, 059 (2018)
- [92] Julien Baglio, Francisco Campanario, Seraina Glaus *et al.*, [Eur. Phys. J. C](#) **79**(6), 459 (2019)
- [93] Long-Bin Chen, Hai Tao Li, Hua-Sheng Shao *et al.*, [Phys. Lett. B](#) **803**, 135292 (2020)
- [94] Long-Bin Chen, Hai Tao Li, Hua-Sheng Shao *et al.*, [JHEP](#) **03**, 072 (2020)
- [95] Alexandra Carvalho, Martino Dall'Osso, Tommaso Dorigo *et al.*, [JHEP](#) **04**, 126 (2016)
- [96] Alexandra Carvalho, Martino Dall'Osso, Pablo De Castro Manzano *et al.*, *Analytical parametrization and shape classification of anomalous HH production in the EFT approach. 7* (2016)
- [97] Adam Alloul, Neil D. Christensen, Céline Degrande *et al.*, [Comput. Phys. Commun.](#) **185**, 2250-2300 (2014)
- [98] Celine Degrande, Claude Duhr, Benjamin Fuks *et al.*, [Comput. Phys. Commun.](#) **183**, 1201-1214 (2012)
- [99] Thomas Hahn, [Comput. Phys. Commun.](#) **140**, 418-431 (2001)
- [100] Celine Degrande, [Comput. Phys. Commun.](#) **197**, 239-262 (2015)
- [101] J. Alwall, R. Frederix, S. Frixione *et al.*, [JHEP](#) **07**, 079 (2014)
- [102] Andy Buckley, James Ferrando, Stephen Lloyd *et al.*, [Eur. Phys. J. C](#) **75**, 132 (2015)
- [103] Valentin Hirschi and Olivier Mattelaer, [JHEP](#) **10**, 146 (2015)
- [104] Albert M Sirunyan *et al.*, [Phys. Rev. Lett.](#) **122**(12), 121803 (2019)
- [105] Georges Aad *et al.*, [Phys. Lett. B](#) **800**, 135103 (2020)
- [106] M. Cepeda *et al.*, *Report from Working Group 2: Higgs Physics at the HL-LHC and HE-LHC*, volume 7, pages 221–584. 12 (2019)
- [107] T. Hahn and M. Perez-Victoria, [Comput. Phys. Commun.](#) **118**, 153-165 (1999)